Article:
Myers, R.J., Provis, J.L., L'Hôpital, E. et al. (1 more author) (2014) Effect of temperature and aluminium on calcium (alumino)silicate hydrate chemistry under equilibrium conditions. Cement and Concrete Research, 68. 83 - 93. ISSN 0008-8846

https://doi.org/10.1016/j.cemconres.2014.10.015

Preprint version of accepted article. Please cite as:
*R.J. Myers, E. L'Hôpital, J.L. Provis, B. Lothenbach, "Effect of temperature and aluminium on calcium (alumino)silicate hydrate chemistry under equilibrium conditions", Cement and Concrete Research **2015**, 68:83-93.*
Official journal version is online at http://dx.doi.org/10.1016/j.cemconres.2014.10.015

Effect of temperature and aluminium on calcium (alumino)silicate hydrate chemistry under equilibrium conditions

Rupert J. Myers [1,2,a], Emilie L'Hôpital [2,b], John L. Provis [1,c], Barbara Lothenbach [2]*

[1] Department of Materials Science and Engineering, University of Sheffield, S1 3JD, Sheffield, United Kingdom

[2] Laboratory for Concrete and Construction Chemistry, EMPA, Dübendorf, 8600, Switzerland

* Corresponding author. Email Barbara.Lothenbach@empa.ch

[a] rjmyers@sheffield.ac.uk. [b] Emilie.Lhopital@empa.ch. [c] j.provis@sheffield.ac.uk.

Keywords

Temperature, Calcium-Silicate-Hydrate (C-S-H), Thermodynamic Calculations, Hydration Products, Blended Cement.

Abstract

There exists limited information regarding the effect of temperature on the structure and solubility of calcium aluminosilicate hydrate (C-A-S-H). Here, calcium (alumino)silicate hydrate (C-(A-)S-H) is synthesised at Ca/Si = 1, Al/Si ≤ 0.15 and equilibrated at 7-80°C.

Preprint version of accepted article. Please cite as:
*R.J. Myers, E. L'Hôpital, J.L. Provis, B. Lothenbach, "Effect of temperature and aluminium on calcium (alumino)silicate hydrate chemistry under equilibrium conditions", Cement and Concrete Research **2015**, 68:83-93.*
Official journal version is online at http://dx.doi.org/10.1016/j.cemconres.2014.10.015

These systems increase in phase-purity, long-range order, and degree of polymerisation of C-(A-)S-H chains at higher temperatures; the most highly polymerised, crystalline and cross-linked C-(A-)S-H product is formed at Al/Si = 0.1 and 80°C. Solubility products for C-(A-)S-H were calculated via determination of the solid-phase compositions and measurements of the concentrations of dissolved species in contact with the solid products, and show that the solubilities of C-(A-)S-H change slightly, within the experimental uncertainty, as a function of Al/Si ratio and temperature between 7°C and 80°C. These results are important in the development of thermodynamic models for C-(A-)S-H to enable accurate thermodynamic modelling of cement-based materials.

1. Introduction

Temperatures experienced by cement and concrete based construction materials in service can vary greatly, due to heat evolution from cement hydration, variable ambient environmental conditions, steam curing, and other factors. The effects of temperature on hydrated blended and neat Portland cement (PC) material properties are important, and can include: increased reaction rate and density of calcium silicate hydrate (C-S-H) [a] [1], coarsening of paste microstructures [2], and decreasing compressive strengths [3] with increasing temperature. Despite the wealth of engineering information available in this area, only a few studies are available in the literature regarding the equilibrium phase assemblages and aqueous chemistry of PC systems as a function of temperature [1, 4, 5]. However, a good

[a] Cement chemistry shorthand notation is used throughout the text: A, Al_2O_3; C, CaO; H, H_2O; and S, SiO_2.

understanding of the nature of C-S-H and other constituent phases in these systems at equilibrium [6-9] has meant that hydrated neat PC materials can be accurately described by thermodynamic modelling at temperatures from 5°C to above 80°C [10]. Extending this analysis to the CaO-Al_2O_3-SiO_2-H_2O system represents a major step toward applying this technique to hydrated PC blends with high replacement levels of supplementary cementitious materials, which are not fully described by existing thermodynamic models [11]. This will enable a much deeper understanding of the chemistry and phase composition, and hence durability, of these materials in service.

The chemistry and structure of calcium (alumino)silicate hydrate (C-(A-)S-H) products at ambient conditions have been the subject of sustained research for more than half a century [12]. These products are structurally similar to the tobermorite group of minerals, which contain aluminosilicate chains in 'dreierketten'-type arrangements that are flanked on either side by an 'interlayer' region and a calcium oxide sheet (Figure 1) [13, 14]. Al substitutes into bridging sites with strong preference over paired sites in these chains [15, 16]. It has also been suggested that the aluminosilicate chains in C-(A-)S-H products can cross-link in low-Ca (Ca/Si < 1) cements [17] to form disordered analogues of 'double chain' calcium silicate minerals, e.g. 11Å tobermorite [18] (Figure 1A).

Preprint version of accepted article. Please cite as:
R.J. Myers, E. L'Hôpital, J.L. Provis, B. Lothenbach, "Effect of temperature and aluminium on calcium (alumino)silicate hydrate chemistry under equilibrium conditions", Cement and Concrete Research ***2015****, 68:83-93.*
Official journal version is online at http://dx.doi.org/10.1016/j.cemconres.2014.10.015

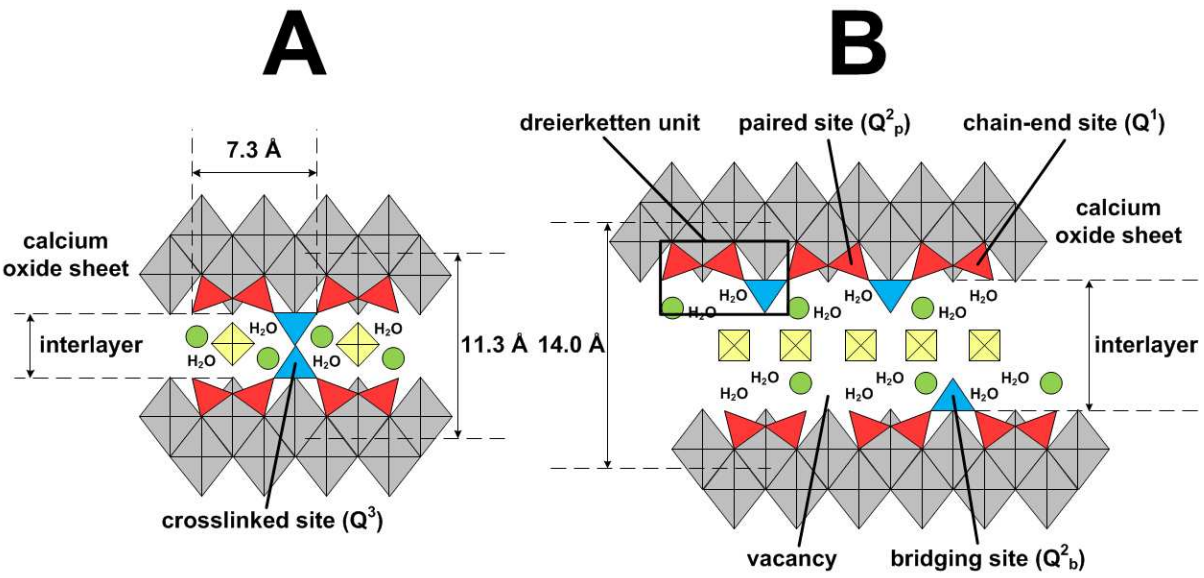

Figure 1. Schematic representation of the nanostructures of finite chain length A) cross-linked and B) non-cross-linked C-(A-)S-H products as structural analogues of double chain 11 Å tobermorite [18] and 14 Å tobermorite [13] respectively. The grey diamonds are Ca species in the Ca-O sheet, and red and blue triangles are aluminosilicate units in paired and bridging sites respectively. The green circles and yellow squares represent sites which can be occupied by positively-charged species that charge-neutralise the structure as a whole (typically H^+, Ca^{2+} and/or alkali species such as K^+ or Na^+).

Studies analysing laboratory-synthesised C-(A-)S-H specimens have identified that phase-purity decreases as the Al/Si and Ca/(Al+Si) molar ratios of the solid phase increase, suggesting that a 'soft' upper bound on the Al content of C-(A-)S-H exists in the composition range relevant to cementitious materials of Al/Si ≈ 0.2 [19-21]. The secondary phases formed in these systems are typically AFm (Al_2O_3-Fe_2O_3-mono) type phases such as strätlingite (C_2ASH_8), katoite (C_3AH_6, which is the Si-free end member of the hydrogarnet series $C_3AS_yH_{6-2y}$, $0 \leq y \leq 3$) and/or the 'third aluminate hydrate' (TAH) [19, 21].

Considering the aqueous phases in equilibrium with C-(A-)S-H at different temperatures, it has been observed that the dissolved concentrations of Ca and Si are inversely related [20, 21], similar to the solubility of these elements in C-S-H systems [22, 23]. The dissolved Al content is closely linked to the amount of Al incorporated into C-(A-)S-H, and the nature and

quantity of secondary phases formed. However, more experimental work is needed to provide data covering the full range of compositions and temperatures relevant to modern cementitious materials. Therefore, this paper aims to clarify the effects of temperature and Al on the chemistry, structure and solubility of equilibrated C-(A-)S-H systems at 7°C, 50°C and 80°C, which are not yet well-described in the literature, and also utilises a recently published data set collected at 20°C [21] to complete the temperature series.

2. Materials and methods

C-(A-)S-H samples were prepared by mixing Milli-Q water (Merck Millipore), SiO_2 (Aerosil 200, Evonik), CaO (obtained by burning $CaCO_3$ (Merck Millipore) at 1000°C for 12 hours) and $CaO{\cdot}Al_2O_3$ at a water/solid ratio of 45 in an N_2-filled glovebox to obtain bulk molar Al/Si ratios (Al/Si*) of 0 to 0.15, with all experiments conducted at a bulk Ca/Si ratio of 1. The $CaO{\cdot}Al_2O_3$ (99.1 wt.% determined by X-ray diffraction (XRD) with Rietveld analysis) was made from $CaCO_3$ and Al_2O_3 (Sigma Aldrich) by heating for 1 hour at 800°C, 4 hours at 1000°C and 8 hours at 1400°C in a Carbolite HTF 1700 furnace (the heating rate to 800°C and between each subsequent temperature was 300°C/hour), then cooled at 600°C/hour under laboratory atmosphere and ground with a Retsch PM100 ball mill to a Blaine surface area of 3790 cm^2/g [24]. Samples were equilibrated at 7°C, 20°C and 50°C in polyethylene vessels and at 80°C in Teflon vessels. The 7°C, 50°C and 80°C samples were shaken twice per week and the 20°C samples were shaken continuously at 100 rpm. Once equilibrium was approached (1 year at 7°C, 182 days at 20°C, and 56 days at 50°C and 80°C), the samples were vacuum filtered with 0.45 µm nylon filters in a N_2-filled glovebox. Equilibration times were selected following the study of C-(A-)S-H kinetics at 20°C in [21], which showed

approximately constant supernatant compositions after 182 days; additional analysis generally showed small differences (< ±25%) in dissolved Si, Al and Ca concentrations between 91 days and 1 year for the 7°C samples and 56 and 91 days for the 50°C samples. The filtered solids were washed with a 50% v/v water-ethanol solution, followed by a >94 vol.% ethanol solution, and then freeze-dried for 7 days. The dried solids were stored in N_2-filled desiccators with humidity and CO_2 traps made from saturated $CaCl_2$ solutions (~30% relative humidity, RH) and solid NaOH pellets, until analysis.

A Dionex DP ICS-3000 ion chromatograph was used to determine Ca, Si and Al concentrations in the filtrates (relative measurement error ±10% in the concentration range of interest and detection limit of 0.1 ppm). Si was detected using a sodium carbonate/bicarbonate eluent and a postcolumn reagent of sodium molybdate/sodium lauryl sulphate in metasulfonic acid. Al was measured using a HCl eluent and a Tiron/ammonium acetate postcolumn reagent. Aqueous hydroxide concentrations were determined at ~23°C with a Knick pH meter (pH-Meter 766) equipped with a Knick SE100 electrode that was calibrated against KOH solutions of known concentrations. Thermogravimetric analysis (TGA) data were recorded on a Mettler Toledo TGA/SDTA851^e at a heating rate of 20°C/min under an N_2 atmosphere. Mass losses between 30°C and 550°C were assigned to the combined dehydration and dehydroxylation effects of C-(A-)S-H, katoite, $Al(OH)_3$ and strätlingite products during firing. Powder XRD patterns were recorded on a PANalytical X'Pert Pro MDF diffractometer equipped with a Ge(111) Johansson monochromator for Cu Kα radiation, and an X'Celerator detector, and a step size of 0.017° 2θ. An external CaF_2 standard was used for Rietveld analysis, enabling quantification of the amount of C-(A-)S-H in each sample [25]. Average basal ($d_{(002)}$) spacings of the C-(A-)S-H products were determined by visual inspection. Solid-state ^{29}Si magic angle spinning nuclear magnetic

Preprint version of accepted article. Please cite as:
*R.J. Myers, E. L'Hôpital, J.L. Provis, B. Lothenbach, "Effect of temperature and aluminium on calcium (alumino)silicate hydrate chemistry under equilibrium conditions", Cement and Concrete Research **2015**, 68:83-93.*
Official journal version is online at http://dx.doi.org/10.1016/j.cemconres.2014.10.015

resonance (MAS NMR) spectra were collected for the Al/Si* = 0 and Al/Si* = 0.1 samples at 79.49 MHz on a Bruker Avance 400 MHz NMR spectrometer with a 7 mm CP/MAS probe. The measurements were recorded using a 4500 Hz spinning rate, 9216 scans, π/3 pulses of 2.5 μs, and 20 s relaxation delays. ^{29}Si chemical shifts were referenced to external tetramethylsilane. Spectral deconvolutions were carried out using component peaks with a Lorentzian/Gaussian ratio = 0.5, full width at half height ≤ 3 ppm, constant chemical shifts for each peak, and constrained peak amplitudes, as described in Appendix S1 (Electronic Supporting Information).

Thermodynamic modelling was performed in the GEM Selektor v.3 software (http://gems.web.psi.ch/) [26, 27] using the PSI/Nagra 12/07 thermodynamic database [28], which is updated from [29] via the inclusion of two additional dissolved (alumino)silicate species, and the CEMDATA07 thermodynamic database [9, 10, 30-35] updated to include recently published data for $Al(OH)_3$ and hydrogarnet phases [24, 36]. Solubility products (K_{so}) for C-(A-)S-H, and effective saturation indices (SI*) for relevant solid phases, were calculated from experimental data obtained here. Activity coefficients were calculated using the extended Debye-Hückel equation (in Truesdell-Jones form) with ion size and extended term parameter for KOH ($\dot{a}$ = 3.67 Å and b_γ = 0.123 kg/mol) [37]. The thermodynamic properties of the aqueous species and solid phases used in these calculations are shown in Appendix A.

Preprint version of accepted article. Please cite as:
R.J. Myers, E. L'Hôpital, J.L. Provis, B. Lothenbach, "Effect of temperature and aluminium on calcium (alumino)silicate hydrate chemistry under equilibrium conditions", Cement and Concrete Research ***2015****, 68:83-93.*
Official journal version is online at http://dx.doi.org/10.1016/j.cemconres.2014.10.015

3. Results and discussion

3.1. X-ray powder diffraction with Rietveld analysis

The XRD results show that C-(A-)S-H phases are the dominant reaction products in each sample (Figure 2). Katoite (C_3AH_6, PDF# 00-024-0217) and strätlingite (C_2ASH_8, PDF# 00-029-0285) are also observed in some systems. Siliceous hydrogarnet ($C_3AS_yH_{6-2y}$, $0 < y \leq 3$) is not identified in any of the samples. Katoite and strätlingite are more commonly found as secondary products in the systems with higher bulk Al/Si ratios and lower equilibration temperatures: strätlingite and katoite are observed in every Al-containing system at 7°C, but these phases are only observed in the Al/Si* ≥ 0.1 samples at 20°C, and only katoite is identified in the Al/Si* ≥ 0.1 samples at 50°C. Small amounts of katoite are also found in the Al/Si* = 0.15, 80°C sample. Calcite ($CaCO_3$, PDF# 00-005-0586) is identified in some samples, which is attributed to minor carbonation during sample preparation, storage and/or analysis.

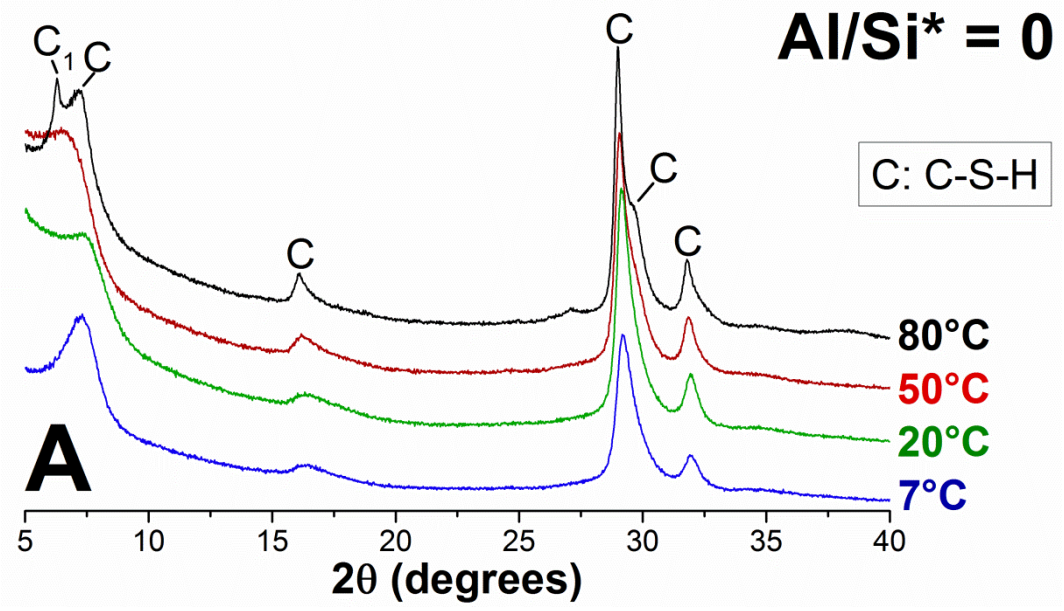

Preprint version of accepted article. Please cite as:
R.J. Myers, E. L'Hôpital, J.L. Provis, B. Lothenbach, "Effect of temperature and aluminium on calcium (alumino)silicate hydrate chemistry under equilibrium conditions", Cement and Concrete Research ***2015****, 68:83-93.*
Official journal version is online at http://dx.doi.org/10.1016/j.cemconres.2014.10.015

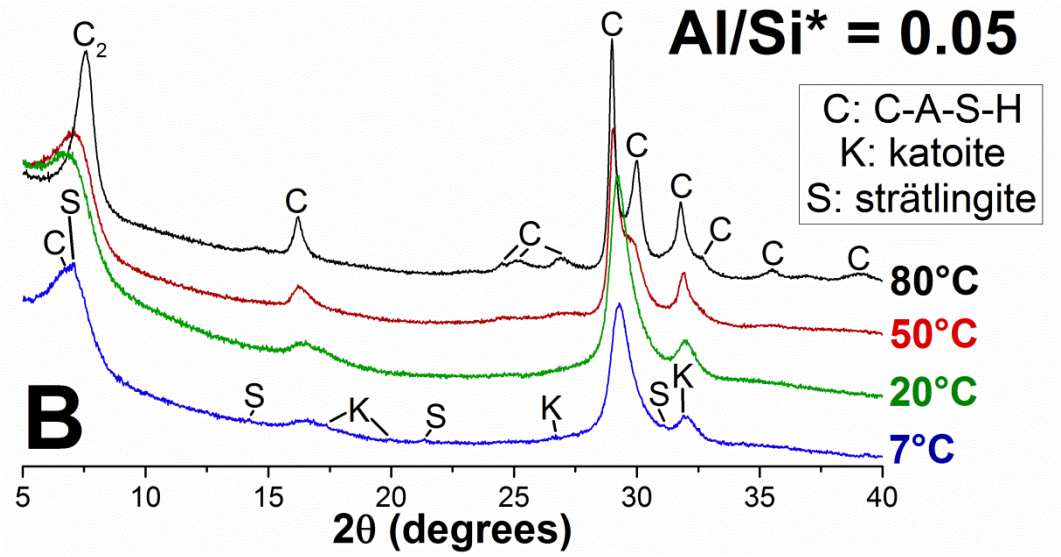

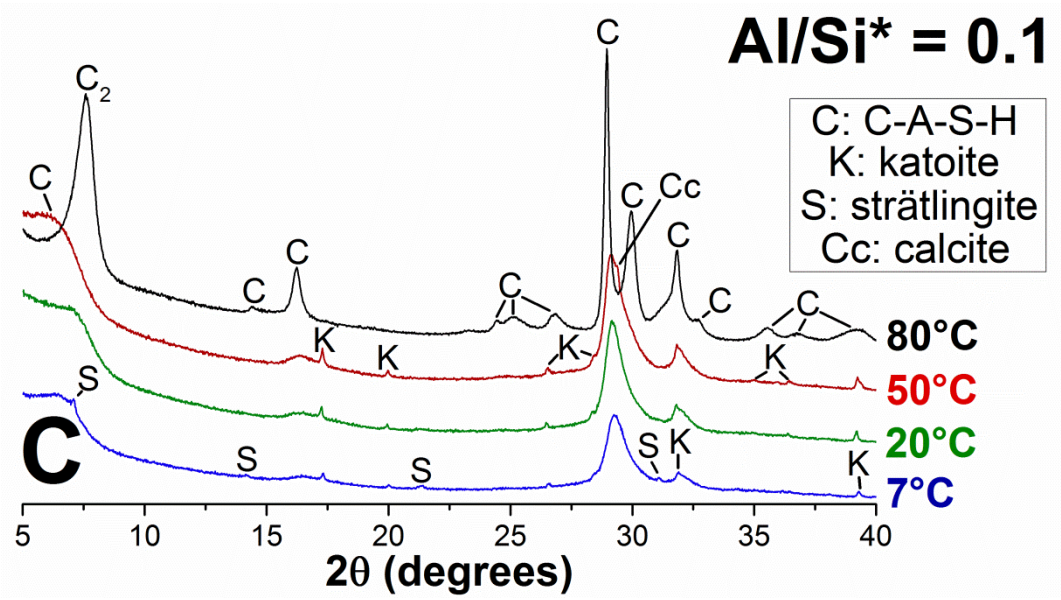

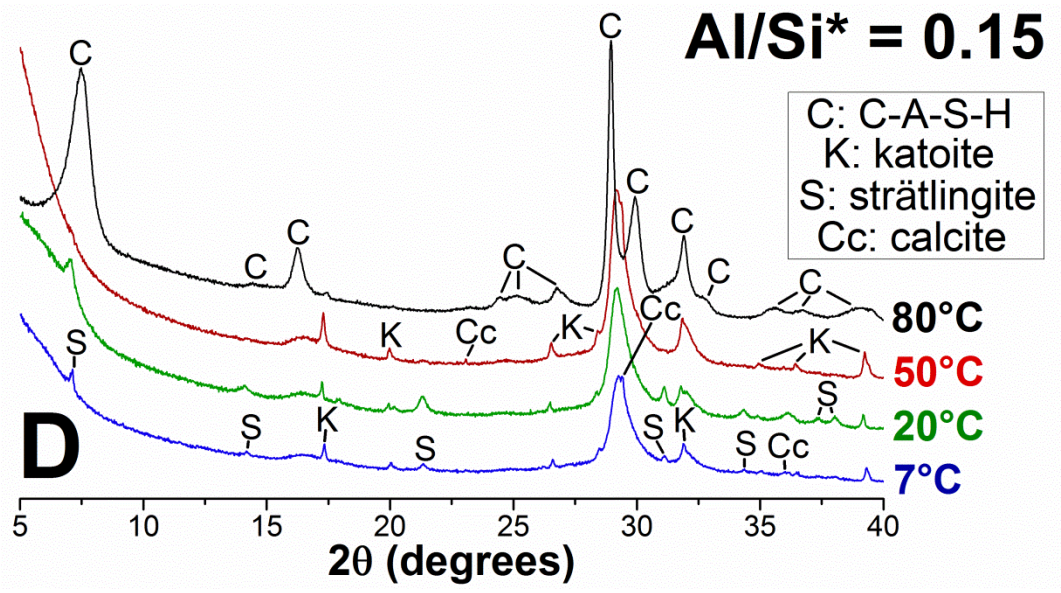

Preprint version of accepted article. Please cite as:
*R.J. Myers, E. L'Hôpital, J.L. Provis, B. Lothenbach, "Effect of temperature and aluminium on calcium (alumino)silicate hydrate chemistry under equilibrium conditions", Cement and Concrete Research **2015**, 68:83-93.*
Official journal version is online at http://dx.doi.org/10.1016/j.cemconres.2014.10.015

Figure 2. Cu Kα diffractograms of the A) C-S-H, and B) Al/Si* = 0.05, C) Al/Si* = 0.1 and D) Al/Si* = 0.15 C-A-S-H systems. Data at 20°C are reproduced from [21]. The peaks marked by C_1 and C_2 represent C-(A-)S-H products with average basal spacings similar to 14 Å tobermorite and 11 Å tobermorite respectively, and C represents C-(A-)S-H products with similarities to both tobermorite types. There is an additional unassigned minor peak at ~43° 2θ in the trace for the Al/Si = 0.1, 7°C sample (not shown). Al/Si* = bulk Al/Si.

The long-range order of the C-(A-)S-H products formed, as identified particularly by the intensity and sharpness of the reflections below 8° 2θ and at ~16° 2θ (Figure 2), increases as a monotonic function of temperature and Al content, to a maximum at Al/Si* = 0.1 or 0.15, and a temperature of 80°C. The peaks for the C-(A-)S-H products correspond to poorly-ordered structural analogues of 14 Å tobermorite ($5CaO{\cdot}6SiO_2{\cdot}9H_2O$, PDF# 00-029-0331), and 11 Å tobermorite ($4.5CaO{\cdot}6SiO_2{\cdot}5.5H_2O$, PDF# 01-074-2784) [18]. These phases can be differentiated in the diffractograms by their different basal spacings; peaks marked C_1 and C_2 in Figure 2 correspond to C-(A-)S-H products with basal spacings that match closely to the (002) reflections for the 14 Å and 11 Å reference tobermorite patterns used here, respectively. The peaks simply marked C indicate reflections of C-(A-)S-H phases with structural similarities to both 14 Å and 11 Å reference tobermorite types. These assignments are consistent with the analysis in [38], where mixtures of 11 Å and 14 Å tobermorite-like structures could best explain the observed shifts of the (002) reflections in the diffractograms of C-S-H systems over the composition range $0.6 < Ca/Si < 1.8$. The average (002) spacings that correspond to the positions of the reflections in the XRD results here do not vary systematically with equilibration temperature or Al/Si ratio, and are between 11 Å and 14 Å for each system studied (Table 1).

Preprint version of accepted article. Please cite as:
*R.J. Myers, E. L'Hôpital, J.L. Provis, B. Lothenbach, "Effect of temperature and aluminium on calcium (alumino)silicate hydrate chemistry under equilibrium conditions", Cement and Concrete Research **2015**, 68:83-93.*
Official journal version is online at http://dx.doi.org/10.1016/j.cemconres.2014.10.015

Table 1. Average ($d_{(002)}$) basal spacings and solid phase assemblages of the C-(A-)S-H systems, determined from Rietveld analysis. Data at 20°C are reproduced from [21]. The estimated absolute error is ±2 wt.% for the secondary products. Al/Si* = bulk Al/Si.

Al/Si * = 0					
Temperature (°C)	**Average basal spacing, $d_{(002)}$ (Å)**	**C-S-H (wt. %)**	**Katoite (wt. %)**	**Strätlingite (wt. %)**	**Calcite (wt. %)**
7	12.1	100	0	0	0
20	11.9	100	0	0	0
50	12.9	100	0	0	0
80	12.1, 14.0 [a]	100	0	0	0
Al/Si* = 0.05					
Temperature (°C)	**Average basal spacing, $d_{(002)}$ (Å)**	**C-A-S-H (wt. %)**	**Katoite (wt. %)**	**Strätlingite (wt. %)**	**Calcite (wt. %)**
7	12.6	99	0.4	0.6	0
20	12.8	100	0	0	0
50	12.3	100	0	0	0
80	11.6	100	0	0	0
Al/Si* = 0.1					
Temperature (°C)	**Average basal spacing, $d_{(002)}$ (Å)**	**C-A-S-H (wt. %)**	**Katoite (wt. %)**	**Strätlingite (wt. %)**	**Calcite (wt. %)**
7	13.1	98.8	0.8	0.4	0
20	12.4	97.2	2.8	0	0
50	13.6	97.6	1.9	0	0.5
80	11.6	100	0	0	0
Al/Si* = 0.15					
Temperature (°C)	**Average basal spacing, $d_{(002)}$ (Å)**	**C-A-S-H (wt. %)**	**Katoite (wt. %)**	**Strätlingite (wt. %)**	**Calcite (wt. %)**
7	-	96.1	2.1	1.4	0.4
20	-	93.4	2.2	4.5	0
50	-	98.5	1.3	0	0.2
80	11.8	99.7	0.3	0	0

[a] Two distinct $d_{(002)}$ reflections were distinguished in the diffractogram of this sample.

Rietveld analysis of the diffractograms indicates that at most only small amounts of secondary products were formed in the systems studied (all samples contained ≥ 93 wt.% C-(A-)S-H, Table 1). Phase purity increased with increasing temperature and decreasing Al content; phase-pure C-S-H was formed in the Al-free systems, and ≥ 99.7 wt.% C-A-S-H was found in the Al-containing samples that were equilibrated at 80°C.

Preprint version of accepted article. Please cite as:
R.J. Myers, E. L'Hôpital, J.L. Provis, B. Lothenbach, "Effect of temperature and aluminium on calcium (alumino)silicate hydrate chemistry under equilibrium conditions", Cement and Concrete Research ***2015****, 68:83-93.*
Official journal version is online at http://dx.doi.org/10.1016/j.cemconres.2014.10.015

3.2. Thermogravimetric analysis

The solid phase assemblages identified in the TGA results (Figure 3) are similar to those identified by XRD (section 3.1); the peaks centred at 80-150°C in the TGA results indicate that >77% of the total mass lost in each sample is from interlayer and structurally bound water in C-(A-)S-H (noting that samples were freeze-dried and equilibrated to ~30% RH to remove the capillary and gel water [39]). The central positions of these mass loss peaks, and the total mass losses in each temperature range, do not vary systematically across the sample synthesis temperature range of 7-80°C, which suggests that the equilibration temperature is not the primary factor controlling the interlayer and structural water content of the C-(A-)S-H products formed here. The relationship between temperature and bound water content in tobermorite [40] and hydrated PC pastes [2] is different; these materials dehydrate progressively with increasing temperature over this temperature range.

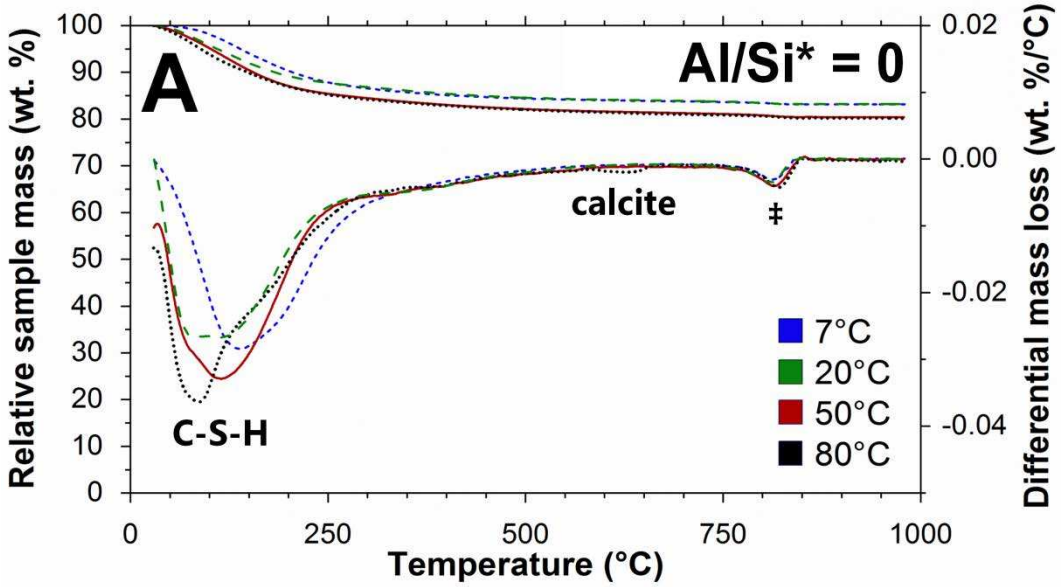

Preprint version of accepted article. Please cite as:
R.J. Myers, E. L'Hôpital, J.L. Provis, B. Lothenbach, "Effect of temperature and aluminium on calcium (alumino)silicate hydrate chemistry under equilibrium conditions", Cement and Concrete Research ***2015****, 68:83-93.*
Official journal version is online at http://dx.doi.org/10.1016/j.cemconres.2014.10.015

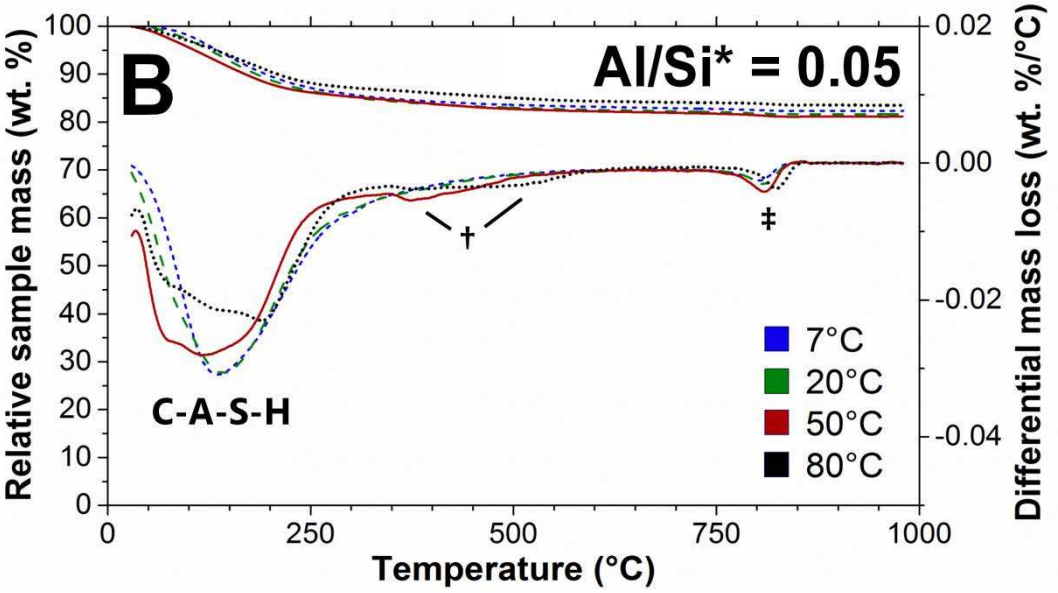

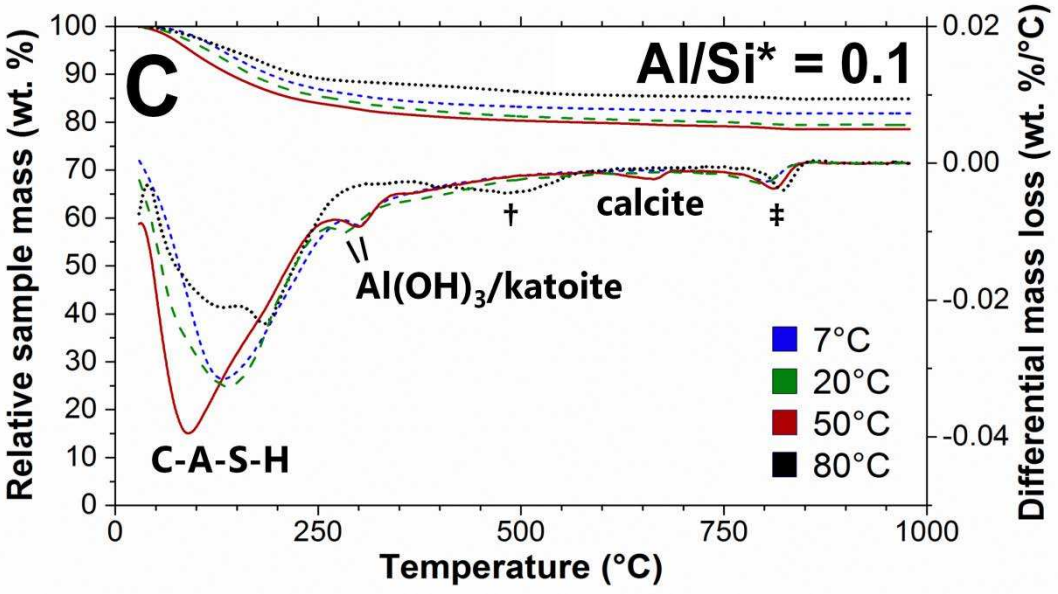

Preprint version of accepted article. Please cite as:
R.J. Myers, E. L'Hôpital, J.L. Provis, B. Lothenbach, "Effect of temperature and aluminium on calcium (alumino)silicate hydrate chemistry under equilibrium conditions", Cement and Concrete Research ***2015****, 68:83-93.*
Official journal version is online at http://dx.doi.org/10.1016/j.cemconres.2014.10.015

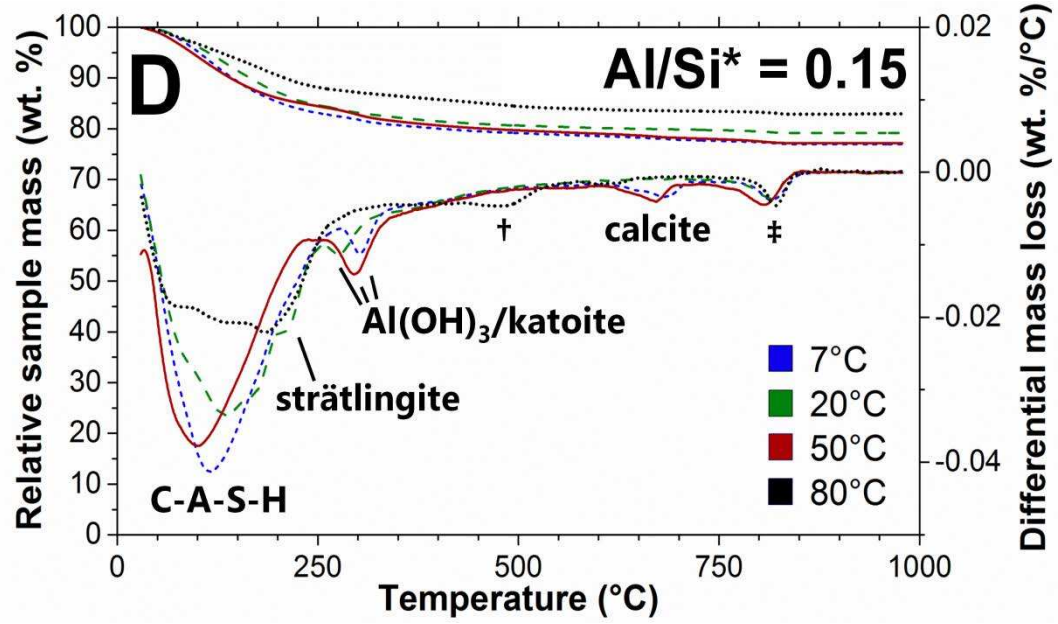

Figure 3. TGA results for the A) C-S-H, and B) Al/Si* = 0.05, C) Al/Si* = 0.1 and D) Al/Si* = 0.15 C-A-S-H systems. Data at 20°C are reproduced from [21]. The data are represented by short-dashed traces at 7°C, long-dashed traces at 20°C, solid traces at 50°C and dotted traces at 80°C. The peaks labelled † and ‡ are assigned to C-(A-)S-H and the decomposition of C-(A-)S-H to wollastonite ($CaSiO_3$), respectively (Appendix S2, Electronic Supporting Information). Al/Si* = bulk Al/Si.

A distinct shoulder at ~200°C is observed in the differential mass loss trace for the Al/Si* = 0.15 sample equilibrated at 20°C (Figure 3D), which is assigned to strätlingite [41]. Small peaks at ~300°C are observed in the differential mass loss traces for the Al/Si* = 0.1 and Al/Si* = 0.15 samples at 7°C and 50°C (Figures 3C-3D), and at ~275°C in the trace for the Al/Si* = 0.1 and Al/Si* = 0.15, 20°C systems. These peaks are assigned to $Al(OH)_3$ at ~275°C and katoite at ~300°C [24]. Minor carbonation during sample preparation, storage and/or analysis is also identified in some samples, by peaks centred at ~650°C.

The derivative mass loss traces for the Al/Si* = 0.05, 50°C sample and the Al/Si* ≥ 0.05, 80°C samples contain wide and shallow peaks at ~380°C and ~500°C (marked by † in Figures 3B-3D). These features are principally affected by equilibration temperature because they are only apparent in the 50°C and 80°C samples, but also appear to be related to Al

content because the band at ~500°C is largest in the Al/Si* = 0.1, 80°C sample compared to the other samples equilibrated at this temperature. These peaks are assigned to thermal decomposition of C-(A-)S-H because none of the additional phases identified by TGA or XRD (section 3.1) can explain the mass losses associated with these bands. The peaks at ~810°C are present in all of the samples studied here (marked by ‡ in Figure 3) and are assigned to the decomposition of C-(A-)S-H to wollastonite ($CaSiO_3$) [42]; wollastonite is known to crystallise from C-S-H [43] and tobermorite [44] at this temperature. Decomposition of C-A-S-H in the temperature range 600-950°C also forms mayenite ($C_{12}A_7$), although distinct differential mass loss peaks for this process are not apparent in Figure 3. Additional XRD data supporting these assignments are shown in Appendix S2 (Electronic Supporting Information).

3.3. Aqueous phase chemistry and C-(A-)S-H chemical composition

Figure 4A shows that the concentrations of Si and OH^- in the supernatant solutions generally increase slightly with increasing temperature in the C-S-H systems (Figure 4A). However, there is not a clear dependence of the measured Ca concentrations on temperature. This result is consistent with published solubility data for C-S-H systems [5, 7, 8, 22, 23, 45-49]. In both the C-S-H (Figure 4A) and C-A-S-H (Figure 4B) samples, the concentrations of Ca, Si and OH^- species in the filtrates change by less than an order of magnitude between 7°C and 80°C (Table S2 in Appendix S3, Electronic Supporting Information).

Preprint version of accepted article. Please cite as:
*R.J. Myers, E. L'Hôpital, J.L. Provis, B. Lothenbach, "Effect of temperature and aluminium on calcium (alumino)silicate hydrate chemistry under equilibrium conditions", Cement and Concrete Research **2015**, 68:83-93.*
Official journal version is online at http://dx.doi.org/10.1016/j.cemconres.2014.10.015

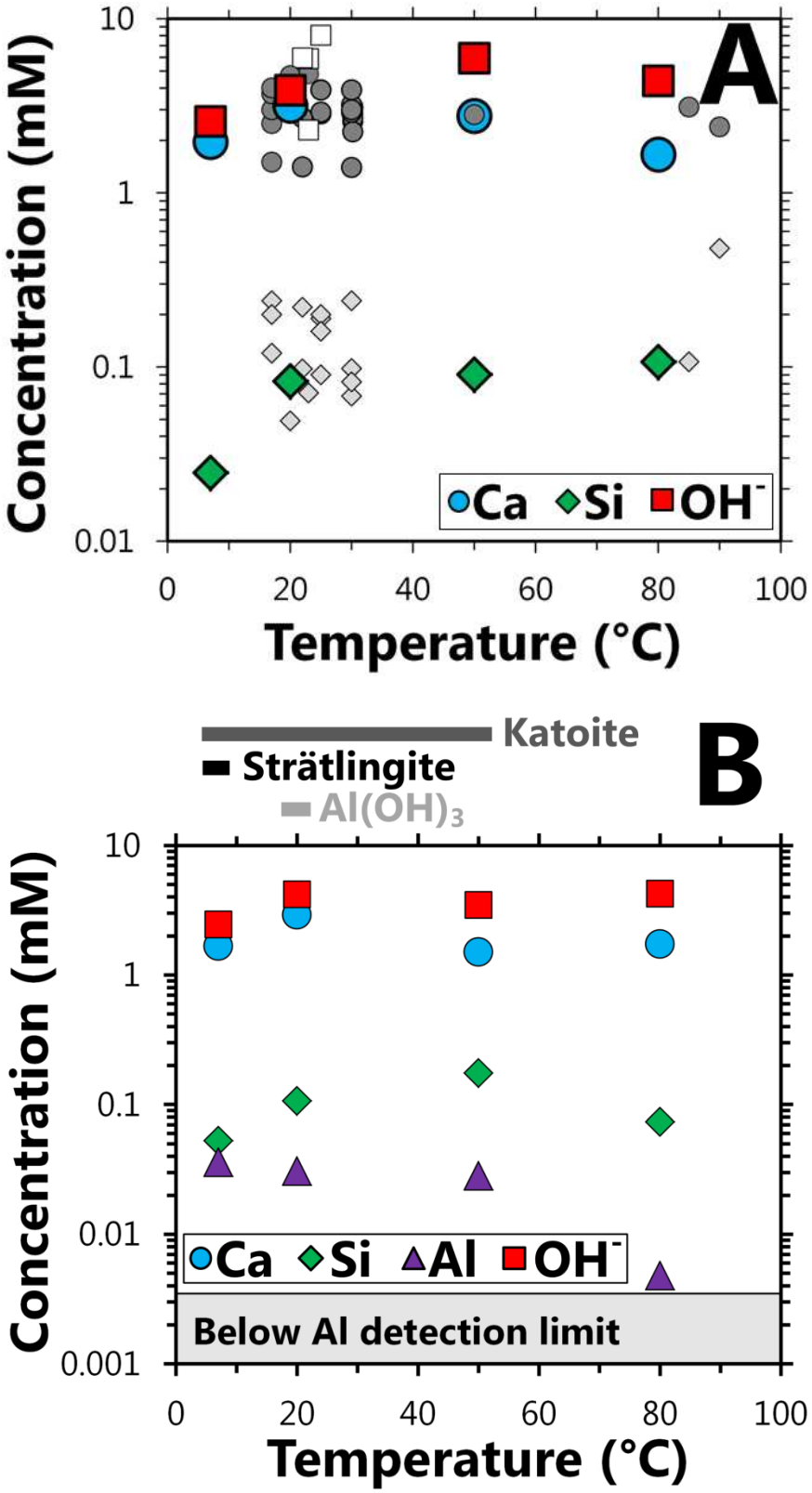

Figure 4. Concentrations of Si, Ca, Al and OH^- species in the filtrates of A) C-S-H and B) C-A-S-H (Al/Si* = 0.1) systems. Data at 20°C are reproduced from [21]. Previously published C-S-H solubility data for systems with solid-phase Ca/Si ratios = 1 ±0.1 [5, 7, 8, 22, 23, 45-49] are shown as small white and grey symbols in A), with shapes corresponding to the

coloured points for the new data. The data measured here (relative error = ±10%) are tabulated in Table S2 (Appendix S3, Electronic Supporting Information). Minor amounts of additional solid products were identified by XRD and TGA in some systems, as marked by horizontal black and grey bars in B).

The C-A-S-H systems, Figure 4B and Appendix S3 (Electronic Supporting Information), show weak increasing trends in the concentrations of dissolved Si and OH^- species as a function of temperature and little variation of aqueous Ca content, which is a similar result to that found for the C-S-H systems (Figure 4A). In general, the concentration of dissolved Al is lower at higher temperatures. An increase in bulk Al/Si ratio generally leads to a higher concentration of dissolved Si and Al, and less Ca and OH^- (Figure 4 and Table S2 in Appendix S3, Electronic Supporting Information). The variation in chemical composition of the C-(A-)S-H products is the main factor contributing to the trends in dissolved Ca, Si, Al and OH^- concentrations, and will be addressed in detail in section 3.4. This result is consistent with the published solubility data for C-S-H, which show the same trends in Ca, Si and OH^- concentrations as functions of Ca/Si in the solid phase [22, 23]. Small amounts of secondary products precipitated in the Al-containing systems (sections 3.1-3.2), and also contribute slightly to the measured solubilities of Ca, Si, Al and OH^- species.

Analysis of C-(A-)S-H solubility from these results is complex because the aqueous Si, Ca, Al and OH^- concentrations do not follow monotonically increasing or decreasing trends, and because the samples with Al/Si ≥ 0.1, and the Al/Si = 0.05, 7°C system, contain additional strätlingite, katoite and/or $Al(OH)_3$ products (see sections 3.1-3.2), meaning that the results do not represent the solubility of C-(A-)S-H alone. Therefore, the measured aqueous phase compositions were used to calculate effective saturation index (*SI**) values for each precipitated phase and for some common solid products in the $CaO\text{-}SiO_2\text{-}Al_2O_3\text{-}H_2O$ system using eq.(1), as shown in Table 2, to clarify the relative solubilities of the solids formed here:

Preprint version of accepted article. Please cite as:
*R.J. Myers, E. L'Hôpital, J.L. Provis, B. Lothenbach, "Effect of temperature and aluminium on calcium (alumino)silicate hydrate chemistry under equilibrium conditions", Cement and Concrete Research **2015**, 68:83-93.*
Official journal version is online at http://dx.doi.org/10.1016/j.cemconres.2014.10.015

$$SI_i^* = \frac{1}{n_i}\log_{10}\left(\frac{IAP_i}{K_{so,i}}\right) \quad (1)$$

where the ion activity product (IAP_i) and solubility product ($K_{so,i}$) refer to the dissociation reactions defined for solid i (Appendix A), and n_i is the total stoichiometric amount of ions in the i^{th} dissociation reaction. Here, n is 3.75 for C-S-H ($C_{1.25}S_{1.25}H_{2.5}$), 3 for CH, 2 for $SiO_{2\,(am)}$, 2 for $Al(OH)_3$, 9 for katoite, 9 for Si-hydrogarnet, and 6 for strätlingite. These calculations define effective supersaturation ($SI_i^* > 0$, precipitation), saturation ($SI_i^* = 0$) and undersaturation ($SI_i^* < 0$, dissolution) states with respect to each phase, in each sample at equilibrium.

Table 2. Effective saturation indices for the relevant reaction products in the C-S-H and C-A-S-H systems, calculated from the solution compositions in Figure 4 and Table S2 (Appendix S3, Electronic Supporting Information). Effective saturation indices marked in bold represent solid phases that are observed in the TGA and/or XRD results of the respective experimental systems. A 'near saturated' condition of $-0.4 \leq SI_i^* < 0$ is assumed, as discussed in the text. Al/Si* = bulk Al/Si.

Al/Si* = 0							
Temperature (°C)	**C-S-H [a]**	**CH**	**$SiO_{2\,(am)}$ [b]**	**$Al(OH)_3$ [c]**	**Katoite**	**Si-hydrogarnet**	**Strätlingite**
7	**-0.4**	-1.4	-1.6	n/a [d]	n/a [d]	n/a [d]	n/a [d]
20	**-0.1**	-0.9	-1.7	n/a [d]	n/a [d]	n/a [d]	n/a [d]
50	**-0.1**	-0.6	-1.7	n/a [d]	n/a [d]	n/a [d]	n/a [d]
80	**-0.2**	-0.6	-1.4	n/a [d]	n/a [d]	n/a [d]	n/a [d]
Al/Si* = 0.05							
Temperature (°C)	**C-S-H [a]**	**CH**	**$SiO_{2\,(am)}$ [b]**	**$Al(OH)_3$ [c]**	**Katoite**	**Si-hydrogarnet**	**Strätlingite**
7	**-0.3**	-1.4	-1.5	-0.5	**-1.1**	-0.6	**-0.4**
20	**0.0**	-0.9	-1.6	-0.8	-0.8	-0.3	-0.3
50	**-0.1**	-0.7	-1.6	-1.3	-0.9	-0.4	-0.7
80	**-0.2**	-0.6	-1.5	b.d.l. [e]	b.d.l. [e]	b.d.l. [e]	b.d.l. [e]
Al/Si* = 0.1							
Temperature (°C)	**C-S-H [a]**	**CH**	**$SiO_{2\,(am)}$ [b]**	**$Al(OH)_3$ [c]**	**Katoite**	**Si-hydrogarnet**	**Strätlingite**

Preprint version of accepted article. Please cite as:
*R.J. Myers, E. L'Hôpital, J.L. Provis, B. Lothenbach, "Effect of temperature and aluminium on calcium (alumino)silicate hydrate chemistry under equilibrium conditions", Cement and Concrete Research **2015**, 68:83-93.*
Official journal version is online at http://dx.doi.org/10.1016/j.cemconres.2014.10.015

7	**-0.3**	-1.5	-1.4	-0.3	**-1.1**	-0.5	**-0.4**
20	**-0.1**	-0.9	-1.7	**-0.7**	**-0.8**	-0.3	-0.3
50	**-0.1**	-0.8	-1.4	-0.7	**-0.8**	-0.3	-0.4
80	**-0.3**	-0.6	-1.5	-1.2	-0.9	-0.4	-0.8

Al/Si* = 0.15

Temperature (°C)	C-S-H [a]	CH	$SiO_{2\ (am)}$ [b]	$Al(OH)_3$ [c]	Katoite	Si-hydrogarnet	Strätlingite
7	**-0.4**	-1.6	-1.3	-0.2	**-1.2**	-0.6	**-0.4**
20	**0.0**	-1.1	-1.3	**-0.7**	**-1.0**	-0.4	**-0.3**
50	**-0.1**	-1.0	-1.1	-0.5	**-0.9**	-0.3	-0.3
80	**-0.3**	-0.8	-1.4	-0.6	**-0.8**	-0.3	-0.5

[a] C-S-H is represented here by the mean chain length (MCL) = 5 end-member of the 'downscaled CSH3T model' (Ca/Si = 1, Al/Si = 0) [11].
[b] Amorphous SiO_2.
[c] Microcrystalline $Al(OH)_3$ at 7°C, 20°C and 50°C, and gibbsite at 80°C [24].
[d] n/a = not applicable (systems contain no Al).
[e] Dissolved Al concentration is below the detection limit (b.d.l.).

The effective saturation indices (Table 2) show that the supernatant solutions are near saturated ($-0.4 \leq SI_i^* < 0$) with respect to C-S-H, and undersaturated with respect to $Ca(OH)_2$ and SiO_2, which is consistent with the solid phase assemblages observed experimentally in these systems (sections 3.1-3.2). The 'near-saturation' range of SI_i^* values chosen here represents the uncertainty associated with both concentration determinations and solubility calculations.

The effective saturation indices (Table 1) indicate that C-S-H is the solid phase most likely to precipitate in each of the Al-free systems. The filtrates in the Al-containing systems are near saturated with respect to C-S-H in each of the systems studied, with respect to $Al(OH)_3$ at 7°C and higher Al concentrations, with respect to strätlingite (C_2ASH_8) at temperatures ≤ 50°C and bulk Al/Si ratios ≥ 0.05, and with respect to Si-hydrogarnet ($C_3AS_{0.84}H_{4.32}$) at temperatures ≥ 20°C and bulk Al/Si ≥ 0.05, which suggests that the systems are close to equilibrium. Katoite (C_3AH_6) was calculated to be undersaturated in each simulated system, although small amounts of this phase were identified in some of the Al-containing systems

(sections 3.1-3.2), which indicates that katoite forms initially from $CaO \cdot Al_2O_3$, CaO and H_2O and that the dissolution of this phase is kinetically hindered. Similar observations have been reported for laboratory-synthesised C-(A-)S-H samples aged for more than 1 year at 20°C [21]. These results suggest that the solid phase assemblages in the CaO-Al_2O_3-SiO_2-H_2O systems studied here are likely to contain several Al-containing solid products at equilibrium. However, the solid phase assemblages found in the experimental samples are dominated by C-(A-)S-H (sections 3.1-3.2), which suggests that this phase outcompetes the other near-saturated phases to form in these systems.

A mass balance was performed using these results, the XRD and Rietveld refinement results and the TGA data, to determine chemical compositions for the C-(A-)S-H products formed in each sample (Table 3). This analysis excluded contributions from $Al(OH)_3$ because no diffraction lines for this phase are present in the XRD results: small mass losses (≤1 wt.%) were associated with $Al(OH)_3$ in the differential mass loss traces for the Al/Si* = 0.1 and Al/Si* = 0.15, 20°C samples only (section 3.2), meaning that any error introduced in the reported C-(A-)S-H compositions by neglecting Al incorporated into this phase, is minor.

Preprint version of accepted article. Please cite as:
*R.J. Myers, E. L'Hôpital, J.L. Provis, B. Lothenbach, "Effect of temperature and aluminium on calcium (alumino)silicate hydrate chemistry under equilibrium conditions", Cement and Concrete Research **2015**, 68:83-93.*
Official journal version is online at http://dx.doi.org/10.1016/j.cemconres.2014.10.015

Table 3. Chemical compositions of the C-S-H and C-A-S-H products, determined from the aqueous phase concentrations, TGA results and Rietveld analysis. Data at 20°C are reproduced from [21]. The estimated absolute errors are ±0.04 units in the Ca/Si ratios, ±0.2 units in the H_2O/Si ratios, and ±0.04 units at 7°C, ±0.03 units at 20°C, ±0.02 units at 50 and 80°C in the Al/Si ratios of the C-(A-)S-H products. Al/Si* = bulk Al/Si.

Al/Si * = 0	
Temperature (°C)	**C-S-H chemical composition**
7	$(CaO)_{0.99}(SiO_2)_1(H_2O)_{1.2}$
20	$(CaO)_{0.98}(SiO_2)_1(H_2O)_{1.5}$
50	$(CaO)_{0.99}(SiO_2)_1(H_2O)_{1.4}$
80	$(CaO)_{0.99}(SiO_2)_1(H_2O)_{1.4}$
Al/Si* = 0.05	
Temperature (°C)	**C-A-S-H chemical composition**
7	$(CaO)_{0.98}(Al_2O_3)_{0.022}(SiO_2)_1(H_2O)_{1.3}$
20	$(CaO)_{0.99}(Al_2O_3)_{0.025}(SiO_2)_1(H_2O)_{1.4}$
50	$(CaO)_{0.99}(Al_2O_3)_{0.025}(SiO_2)_1(H_2O)_{1.4}$
80	$(CaO)_{0.99}(Al_2O_3)_{0.025}(SiO_2)_1(H_2O)_{1.2}$
Al/Si* = 0.1	
Temperature (°C)	**C-A-S-H chemical composition**
7	$(CaO)_{0.98}(Al_2O_3)_{0.045}(SiO_2)_1(H_2O)_{1.3}$
20	$(CaO)_{0.95}(Al_2O_3)_{0.039}(SiO_2)_1(H_2O)_{1.4}$
50	$(CaO)_{0.96}(Al_2O_3)_{0.043}(SiO_2)_1(H_2O)_{1.6}$
80	$(CaO)_{0.99}(Al_2O_3)_{0.050}(SiO_2)_1(H_2O)_{1.1}$
Al/Si* = 0.15	
Temperature (°C)	**C-A-S-H chemical composition**
7	$(CaO)_{0.95}(Al_2O_3)_{0.061}(SiO_2)_1(H_2O)_{1.7}$
20	$(CaO)_{0.94}(Al_2O_3)_{0.051}(SiO_2)_1(H_2O)_{1.5}$
50	$(CaO)_{0.97}(Al_2O_3)_{0.070}(SiO_2)_1(H_2O)_{1.7}$
80	$(CaO)_{0.98}(Al_2O_3)_{0.074}(SiO_2)_1(H_2O)_{1.3}$

The calculated Ca/Si and Al/Si ratios of the C-(A-)S-H products are generally more similar to the bulk conditions used (Ca/Si = 1 and $0 \leq$ Al/Si ≤ 0.15) in the systems with lower Al content and higher temperatures, because these samples typically contain lower amounts of secondary phases. The Al content of the C-(A-)S-H products and the concentrations of Al dissolved in the supernatant solutions are directly related (Figure 5), and both typically increase with increasing bulk Al/Si ratio. In general, the concentration of dissolved Al decreases and the Al/Si ratio of the C-(A-)S-H phase increases as a function of the equilibration temperature.

Preprint version of accepted article. Please cite as:
*R.J. Myers, E. L'Hôpital, J.L. Provis, B. Lothenbach, "Effect of temperature and aluminium on calcium (alumino)silicate hydrate chemistry under equilibrium conditions", Cement and Concrete Research **2015**, 68:83-93.*
Official journal version is online at http://dx.doi.org/10.1016/j.cemconres.2014.10.015

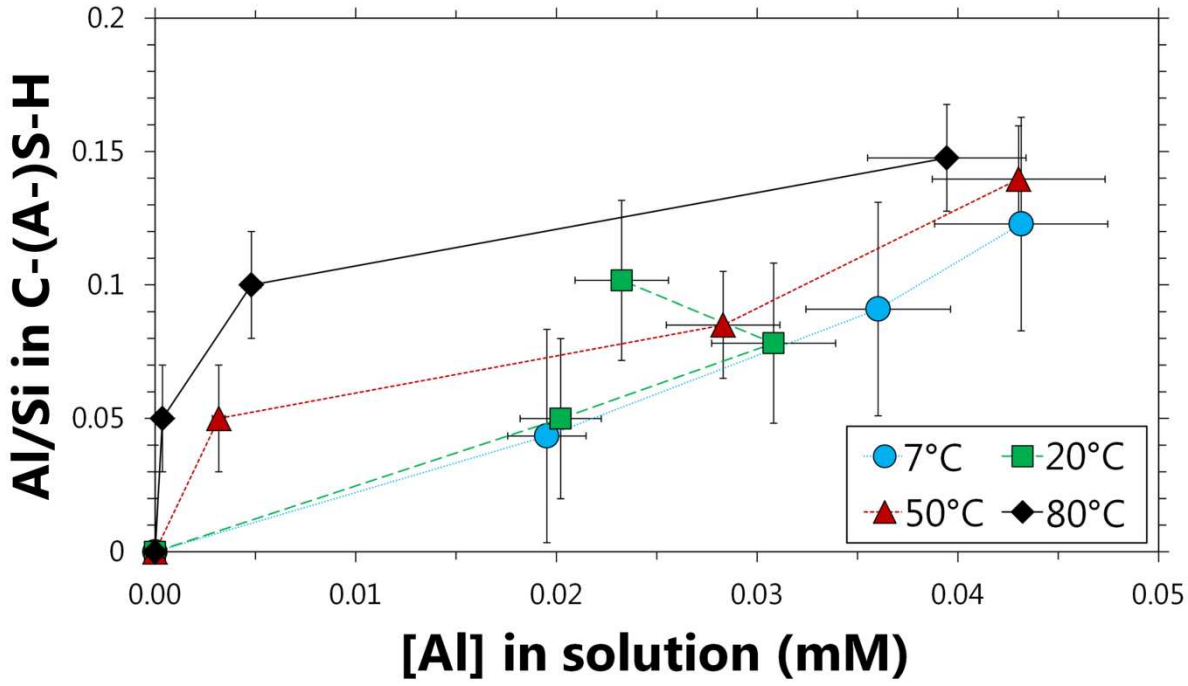

Figure 5. Al/Si ratios of the C-(A-)S-H products as a function of the concentration of Al in the supernatant. Data at 20°C are reproduced from [21]. The uncertainties of the Al/Si ratios calculated for the C-(A-)S-H phases are ±0.04 units at 7°C, ±0.03 units at 20°C, and ±0.02 units at 50 and 80°C. A relative measurement error of ±10% is specified for the aqueous concentrations. Lines are for eye-guides only.

The low water contents determined for the C-(A-)S-H products formed here ($1.1 \leq H_2O/Si \leq 1.7$) compare closely to the proposed values for C-S-H with no adsorbed water ($1.3 \leq H_2O/Si \leq 1.8$ [50, 51]), which suggests that only interlayer and structural water remains after the drying procedure used here (dried to RH ≈ 30% [39]). The use of a more severe drying procedure here than in a recent study of temperature effects on PC pastes [2] explains why the H_2O/Si ratios of the low-Al C-(A-)S-H in that study were found to vary as a function of temperature and were significantly higher ($2.28 \leq H_2O/Si \leq 3.31$) than those determined here.

3.4. ^{29}Si magic angle spinning nuclear magnetic resonance

The ^{29}Si MAS NMR spectra are dominated by intense bands at -79.4 ppm, -83.5 ppm and -85.3 ppm (Figure 6), which are characteristic of silicate species in chain-end (Q^1), bridging

Preprint version of accepted article. Please cite as:
*R.J. Myers, E. L'Hôpital, J.L. Provis, B. Lothenbach, "Effect of temperature and aluminium on calcium (alumino)silicate hydrate chemistry under equilibrium conditions", Cement and Concrete Research **2015**, 68:83-93.*
Official journal version is online at http://dx.doi.org/10.1016/j.cemconres.2014.10.015

(Q^2_b) and paired (Q^2_p) sites respectively (Figure 1) [52]. An additional peak is apparent between the Q^1 and Q^2_p sites in the Al/Si* = 0.1 spectra compared to the Al-free samples, which indicates that Q^2(1Al) sites are present in the C-A-S-H systems. These species lead to bands centred at -81.9 ppm in the deconvoluted spectra [53]. Cross-linked Q^3(1Al) and Q^3 sites are also evident at -91.9 ppm and -96.6 ppm respectively in the spectrum of the Al/Si* = 0.1, 80°C sample, which is the only spectrum that contains clearly visible resonance signals for these sites. Q^3-type sites have also been identified in ^{29}Si MAS NMR spectra of hydrated 60% PC/40% silica fume cements (Ca/Si ≈ 0.83 and Al/Si ≈ 0.035), which were found to increase greatly in intensity at 80°C relative to 20°C and 50°C [54], although these sites are not observed in more Ca-rich materials in this temperature range (e.g. hydrated PC and C_3S [55]). Strätlingite is not explicitly taken into account in deconvolutions of the ^{29}Si MAS NMR spectra; this phase is thought to contain aluminosilicate species with ^{29}Si isotropic chemical shifts of -80 to -90 ppm [56], but is not expected to greatly affect the deconvolution analysis because it was seen to be a minor component via Rietveld analysis for the Al/Si* = 0.1 samples (≤ 0.4 wt.%, Table 1).

Preprint version of accepted article. Please cite as:
R.J. Myers, E. L'Hôpital, J.L. Provis, B. Lothenbach, "Effect of temperature and aluminium on calcium (alumino)silicate hydrate chemistry under equilibrium conditions", Cement and Concrete Research ***2015****, 68:83-93.*
Official journal version is online at http://dx.doi.org/10.1016/j.cemconres.2014.10.015

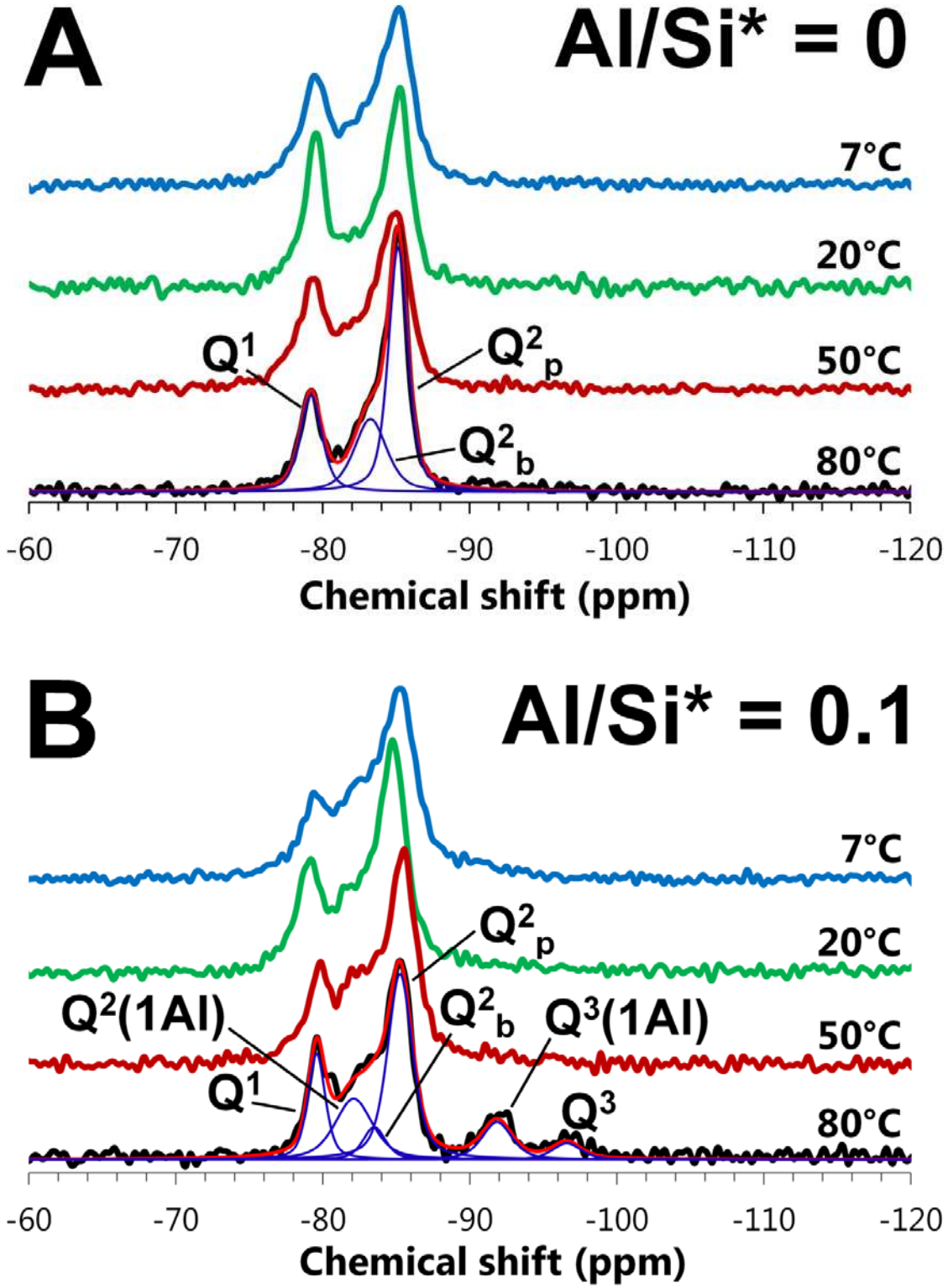

Figure 6. Solid-state ^{29}Si MAS NMR spectra of the A) C-S-H and B) Al/Si* = 0.1 C-A-S-H systems. The fits and deconvoluted peaks for the spectra of the 80°C samples are shown as bright red and blue lines respectively. The chemical shift range corresponding to aluminosilicate sites in strätlingite is approximately -80 to -90 ppm [56]. Data at 20°C are reproduced from [21]. Deconvolutions for each spectrum are shown in Figures S3-S4 (Appendix S4, Electronic Supporting Information). Al/Si* = bulk Al/Si.

Preprint version of accepted article. Please cite as:
*R.J. Myers, E. L'Hôpital, J.L. Provis, B. Lothenbach, "Effect of temperature and aluminium on calcium (alumino)silicate hydrate chemistry under equilibrium conditions", Cement and Concrete Research **2015**, 68:83-93.*
Official journal version is online at http://dx.doi.org/10.1016/j.cemconres.2014.10.015

The lineshapes of the spectra for the samples equilibrated at ≤ 50°C and the same bulk Al/Si ratio are similar, which indicates that the C-(A-)S-H products formed in these samples have similar degrees of polymerisation, as shown in Figure 7, calculated using eq.(2) for non-cross-linked C-(A-)S-H (subscript *NC*) [57]. Al/Si ratios for non-cross-linked C-(A-)S-H are calculated by eq.(3) [57].

$$MCL_{NC} = \frac{2\left[Q^1 + Q^2 + \frac{3}{2}Q^2(1Al)\right]}{Q^1} \quad (2)$$

$$Al/Si_{NC} = \frac{\frac{1}{2}Q^2(1Al)}{Q^1 + Q^2 + Q^2(1Al)} \quad (3)$$

Here, mean chain length (MCL) represents the average number of aluminosilicate tetrahedra per tobermorite-like chain in C-(A-)S-H. The MCL and Al/Si values for cross-linked C-(A-)S-H structures (subscript *C*, i.e. a C-(A-)S-H product containing Q^3 and/or Q^3(1Al) sites) are given by eqs. (4-5) [17]:

$$MCL_C = \frac{4\left[Q^1 + Q^2 + Q^2(1Al) + Q^3 + 2Q^3(1Al)\right]}{Q^1} \quad (4)$$

$$Al/Si_C = \frac{Q^3(1Al)}{Q^1 + Q^2 + Q^2(1Al) + Q^3 + Q^3(1Al)} \quad (5)$$

Preprint version of accepted article. Please cite as:
R.J. Myers, E. L'Hôpital, J.L. Provis, B. Lothenbach, "Effect of temperature and aluminium on calcium (alumino)silicate hydrate chemistry under equilibrium conditions", Cement and Concrete Research ***2015****, 68:83-93.*
Official journal version is online at http://dx.doi.org/10.1016/j.cemconres.2014.10.015

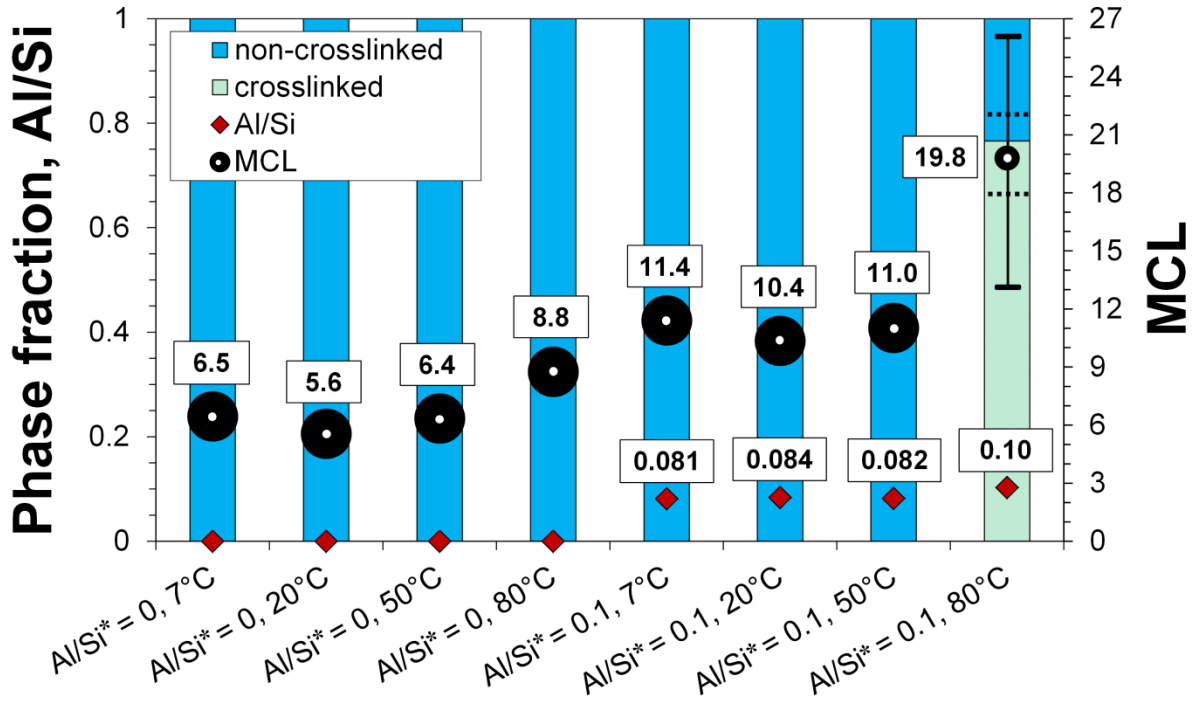

Figure 7. C-(A-)S-H structural parameters calculated from deconvolution analysis of the ^{29}Si MAS NMR spectra, determined using the 'Substituted General Model' [57] for the non-cross-linked phases and the 'Cross-linked Substituted Tobermorite Model' [17] for the cross-linked phases. The sizes of the symbols represent the expected error bounds of the deconvolution results, except for the Al/Si* = 0.1, 80°C sample, where the uncertainty of the MCL calculation is represented by error bars. The cross-linked phase fraction for the C-A-S-H product in this sample has an error bound of +0.05 and -0.1, as marked by the dotted black lines. These results are tabulated in Table S4 (Appendix S4, Electronic Supporting Information). Al/Si* = bulk Al/Si.

The C-(A-)S-H products formed in the samples equilibrated at 80°C are significantly more polymerised than those produced at lower temperatures; the same trend has been reported for C-(A-)S-H products formed in hydrated 60% PC/40% silica fume cements [54]. MCL values of 8.8 and 19.8 ± 6 were calculated for the C-(A-)S-H products in the Al/Si* = 0 and Al/Si* = 0.1 systems at 80°C, respectively. This increase in chain length is associated with a significant increase in the long-range order of the C-(A-)S-H products at 80°C relative to the C-(A-)S-H phases formed at lower temperatures (section 3.1), which is particularly pronounced for the Al-containing samples. The increase in chain polymerisation from 50°C to 80°C is much smaller in the Al-free system relative to the Al/Si* = 0.1 system, and this is

Preprint version of accepted article. Please cite as:
*R.J. Myers, E. L'Hôpital, J.L. Provis, B. Lothenbach, "Effect of temperature and aluminium on calcium (alumino)silicate hydrate chemistry under equilibrium conditions", Cement and Concrete Research **2015**, 68:83-93.*
Official journal version is online at http://dx.doi.org/10.1016/j.cemconres.2014.10.015

consistent with the observation of cross-linked chain structures only in the Al/Si* = 0.1 sample. Therefore, these results indicate that the formation of highly polymerised and cross-linked C-(A-)S-H products is promoted substantially by the presence of Al.

Figure 8 shows that the Al/Si ratios determined from analysis of the ^{29}Si MAS NMR spectral deconvolution results (Figure 7) match closely with the chemical compositions of the C-(A-)S-H products determined independently by the TGA results, measured filtrate compositions and Rietveld analysis (Table 3). The formation of a highly cross-linked C-A-S-H product in the Al/Si* = 0.1, 80°C sample is also consistent with the low average basal spacing for the C-A-S-H phase in this system (11.6 Å, Table 1), which is similar to the layer spacing of double chain 11 Å tobermorite (11.3 Å, Figure 1A).

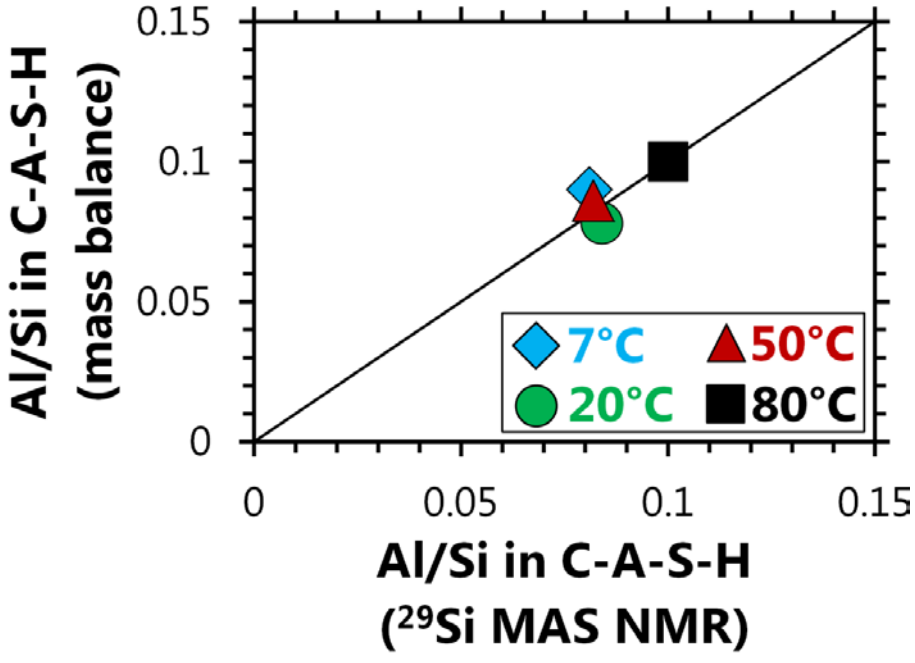

Figure 8. Comparison between the chemical compositions of the C-A-S-H products in the Al/Si* = 0.1 samples, as determined by mass balance (TGA, XRD, aqueous phase compositions – Table 3) and deconvolutions of ^{29}Si MAS NMR spectra (Figure 7). The sizes of the symbols represent the expected uncertainty in the spectral deconvolution results. The solid y = x line is intended as an eye-guide only.

Preprint version of accepted article. Please cite as:
*R.J. Myers, E. L'Hôpital, J.L. Provis, B. Lothenbach, "Effect of temperature and aluminium on calcium (alumino)silicate hydrate chemistry under equilibrium conditions", Cement and Concrete Research **2015**, 68:83-93.*
Official journal version is online at http://dx.doi.org/10.1016/j.cemconres.2014.10.015

3.5. C-(A-)S-H solubility

Solubility products (K_{so}) were calculated for hypothetical C-(A-)S-H end-members with chemical compositions corresponding to the bulk chemistry of the systems studied (Al/Si = 0, 0.05, 0.1, 0.15) but normalised to Ca/(Al+Si) = 1 and H_2O/Si = 1.2, using the reaction represented by eq.(6):

$$(CaO)_a\left(SiO_2\right)_b\left(Al_2O_3\right)_c\left(H_2O\right)_f \xrightleftharpoons{K_{so}} aCa^{2+}{}_{(aq)} + bSiO_3^{2-}{}_{(aq)} + 2cAlO_2^{-}{}_{(aq)} + 2\left(a-b-c\right)OH^{-}{}_{(aq)} + \left(b+c+f-a\right)H_2O_{(l)} \quad (6)$$

where *a*, *b*, *c* and *f* are the respective stoichiometric coefficients for CaO, SiO_2, Al_2O_3 and H_2O in the C-(A-)S-H end-members. This reaction implies the following relationships for K_{so} (eq.(7)):

$$K_{so} = \left\{Ca^{2+}{}_{(aq)}\right\}^a \cdot \left\{SiO_3^{2-}{}_{(aq)}\right\}^b \cdot \left\{AlO_2^{-}{}_{(aq)}\right\}^{2c} \cdot \left\{OH^{-}{}_{(aq)}\right\}^{2(a-b-c)} \cdot \left\{H_2O_{(l)}\right\}^{(b+c+f-a)} \quad (7)$$

Activities of $Ca^{2+}{}_{(aq)}$, $SiO_3^{2-}{}_{(aq)}$, $AlO_2^{-}{}_{(aq)}$, $OH^{-}{}_{(aq)}$ and $H_2O_{(l)}$ were determined in GEM-Selektor (http://gems.web.psi.ch/) [26, 27]; the OH^- concentration was matched to the measured pH values. The results of these calculations, for the hypothetical C-(A-)S-H end-members, are shown in Figure 9. Solubility products were calculated in the same way for the experimental C-(A-)S-H products with chemical compositions determined from the measured supernatant concentrations, TGA data and XRD results (Table 3), which are shown in Table S3 (Appendix S3, Electronic Supporting Information).

Preprint version of accepted article. Please cite as:
R.J. Myers, E. L'Hôpital, J.L. Provis, B. Lothenbach, "Effect of temperature and aluminium on calcium (alumino)silicate hydrate chemistry under equilibrium conditions", Cement and Concrete Research ***2015****, 68:83-93.*
Official journal version is online at http://dx.doi.org/10.1016/j.cemconres.2014.10.015

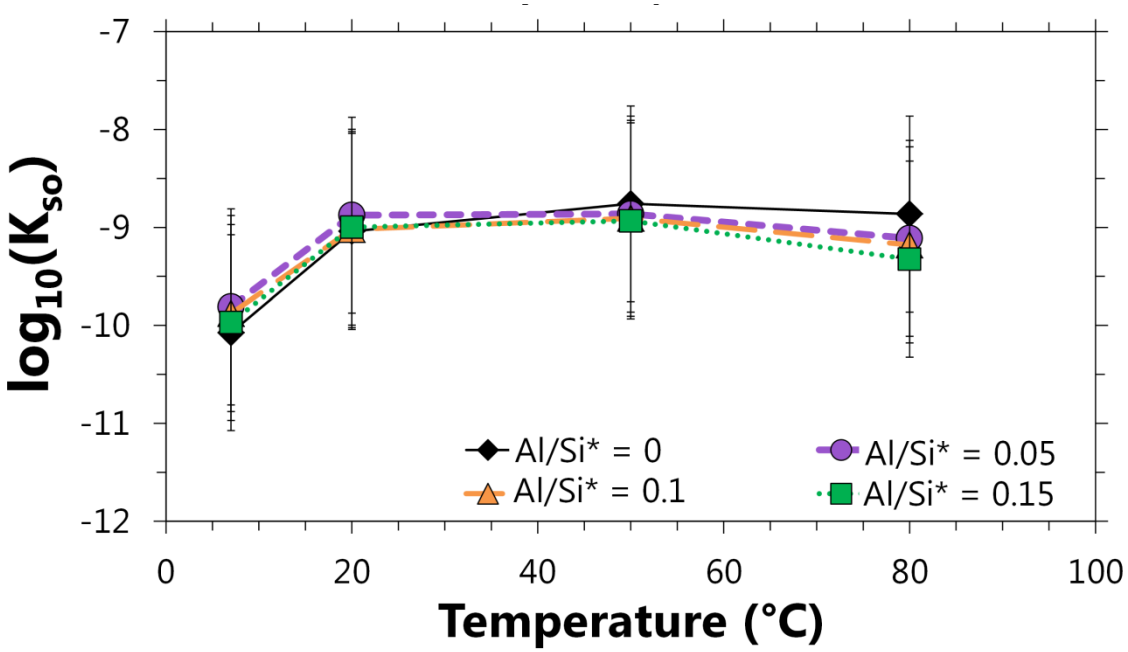

Figure 9. Calculated $\log_{10}(K_{so})$ values for hypothetical C-(A-)S-H end-members with chemical compositions of Ca/(Al+Si) = 1, Al/Si = 0, 0.05, 0.1 and 0.15, and H_2O/Si = 1.2, and normalised to 1 mol SiO_2. The approximate uncertainty in the $\log_{10}(K_{so})$ values are ±1 $\log_{10}$ unit. The solubility product for the C-A-S-H product formed in the Al/Si* = 0.05 sample equilibrated at 80°C was calculated with [Al] = 0.001 mM because the measured Al concentration was below the detection limit. Al/Si* = bulk Al/Si.

The solubility products of the hypothetical C-(A-)S-H end-members change slightly between 7°C and 80°C, and very slightly as a function of Al/Si ratio, but remain within the error bound of ±1 log unit (Figure 9). These solubility products ($-9 < \log_{10}(K_{so}) < -10$) are comparable to those recalculated from reported Ca, Si and OH^- solubilities in laboratory-synthesised Ca/Si = 0.83 tobermorite specimens using eq.(6) (-8.1 ±0.3 at 25°C, -9.3 ±0.6 at 55°C and -9.6 ±0.2 at 85°C [58]), as expected for these structurally and compositionally-similar phases. Despite the large uncertainty relative to the variation in the calculated solubility products, the 80°C data do show a small systematic reduction in C-(A-)S-H solubility as the Al/Si ratio of this phase increases, which could indicate that these phases are slightly stabilised by the incorporation of Al at high temperature, but further experimental

solubility data are necessary to clarify this point. The precipitation of small amounts of katoite, strätlingite and calcite (Table 1) is not expected to significantly affect the trends in C-(A-)S-H solubility reported here, although the results depend slightly on this factor.

Nonetheless, the weak dependency of C-(A-)S-H solubility on temperature, clearly shown by these data, is an important result which will influence the development of thermodynamic models for cementitious materials across the temperature range of interest for the majority of service conditions worldwide.

4. Conclusions

This paper has analysed the structure and solubility of calcium (alumino)silicate hydrates, with and without the inclusion of Al, as a function of temperature. The long-range order and degree of polymerisation of the C-(A-)S-H products, and the type and quantity of secondary phases formed in the equilibrated CaO-Al_2O_3-SiO_2-H_2O systems studied here, were significantly influenced by the synthesis temperature. The supernatants in these systems were close to saturation with respect to strätlingite and $Al(OH)_3$ products at lower temperatures and higher Al/Si ratios, and equilibrium was attained more rapidly at high temperatures, meaning that the Al-free and 80°C systems contained the most phase-pure C-(A-)S-H products. The C-(A-)S-H phases formed at 80°C were much more polymerised and long-range ordered than those produced at 7, 20 and 50°C, and the C-A-S-H product in the 80°C, Al/Si = 0.1 system was also highly cross-linked. However, no Q^3-type sites were evident in the ^{29}Si MAS NMR spectra for the C-S-H formed in the Al-free system at this temperature, indicating that cross-linking in C-(A-)S-H products is promoted by the presence of Al.

Solubility products for the C-(A-)S-H phases formed here did not vary beyond the experimental error bounds as a function of temperature or Al/Si ratio, but a small systematic reduction in C-(A-)S-H solubility at 80°C as the bulk Al/Si ratio was increased could indicate that these phases are slightly stabilised by Al at this temperature. Therefore, this study is an important step towards the development of thermodynamic models for C-A-S-H and advances the application of thermodynamic modelling to C-(A-)S-H based cements across the temperature range 7-80°C, which will provide new insight into the performance of these materials in service.

5. Supporting information

Additional material is provided as Electronic Supporting Information: details of the deconvolution method for the ^{29}Si MAS NMR spectra is provided in Appendix S1; additional details of the differential mass loss peak assignments are shown in Appendix S2 (Figures S1-S2); tabulated data relevant to the thermodynamic modelling calculations, including aqueous phase compositions, are presented in Appendix S3 (Tables S1-S2); and detailed ^{29}Si MAS NMR spectral deconvolution results are provided in Appendix S4 (Figure S3-S4 and Table S3). This material can be accessed via the journal website (http://www.journals.elsevier.com/cement-and-concrete-research/).

Preprint version of accepted article. Please cite as:
*R.J. Myers, E. L'Hôpital, J.L. Provis, B. Lothenbach, "Effect of temperature and aluminium on calcium (alumino)silicate hydrate chemistry under equilibrium conditions", Cement and Concrete Research **2015**, 68:83-93.*
Official journal version is online at http://dx.doi.org/10.1016/j.cemconres.2014.10.015

6. Acknowledgements

The authors thank Salaheddine Alahrache and Daniel Rentsch for assistance with NMR spectroscopy, Luigi Brunetti and Boris Ingold for assistance in the laboratory and the Swiss National Science Foundation grant n° 130419 for the financial support of E. L'Hôpital.

7. References

[1] B. Lothenbach, F. Winnefeld, C. Alder, E. Wieland, P. Lunk, Effect of temperature on the pore solution, microstructure and hydration products of Portland cement pastes, Cem. Concr. Res., 37 (4) (2007) 483-491.

[2] E. Gallucci, X. Zhang, K.L. Scrivener, Effect of temperature on the microstructure of calcium silicate hydrate (C-S-H), Cem. Concr. Res., 53 (2013) 185-195.

[3] J.I. Escalante-García, J.H. Sharp, Effect of temperature on the hydration of the main clinker phases in portland cements: part I, neat cements, Cem. Concr. Res., 28 (9) (1998) 1245-1257.

[4] J.J. Thomas, D. Rothstein, H.M. Jennings, B.J. Christensen, Effect of hydration temperature on the solubility behavior of Ca-, S-, Al-, and Si-bearing solid phases in Portland cement pastes, Cem. Concr. Res., 33 (12) (2003) 2037-2047.

[5] M. Atkins, F. Glasser, L.P. Moroni, J.J. Jack, Thermodynamic modelling of blended cements at elevated temperature (50-90°C), Aberdeen University, United Kingdom, DoE1HMIP1RR/94.011, 1994.

[6] F.P. Glasser, J. Pedersen, K. Goldthorpe, M. Atkins, Solubility reactions of cement components with NaCl solutions: I. $Ca(OH)_2$ and C-S-H, Adv. Cem. Res., 17 (2) (2005) 57-64.

[7] A.C. Courault, Simulation expérimentale des C-S-H dans les bétons modernes: étude de la composition et des propriétés à l'équilibre dans des milieux complexes, Université de Bourgogne, Dijon, 2000.

[8] R. Barbarulo, Comportement des matériaux cimentaires: actions des sulfates et de la température, Université Laval, Québec, 2003.

[9] T. Matschei, B. Lothenbach, F.P. Glasser, Thermodynamic properties of Portland cement hydrates in the system $CaO-Al_2O_3-SiO_2-CaSO_4-CaCO_3-H_2O$, Cem. Concr. Res., 37 (10) (2007) 1379-1410.

[10] B. Lothenbach, T. Matschei, G. Möschner, F.P. Glasser, Thermodynamic modelling of the effect of temperature on the hydration and porosity of Portland cement, Cem. Concr. Res., 38 (1) (2008) 1-18.

[11] D.A. Kulik, Improving the structural consistency of C-S-H solid solution thermodynamic models, Cem. Concr. Res., 41 (5) (2011) 477-495.

[12] G.L. Kalousek, Crystal chemistry of hydrous calcium silicates: I, substitution of aluminum in lattice of tobermorite, J. Am. Ceram. Soc., 40 (3) (1957) 74-80.

[13] E. Bonaccorsi, S. Merlino, A.R. Kampf, The crystal structure of tobermorite 14Å (plombierite), a C-S-H phase, J. Am. Ceram. Soc., 88 (3) (2005) 505-512.

[14] I.G. Richardson, The calcium silicate hydrates, Cem. Concr. Res., 38 (2) (2008) 137-158.

[15] H. Manzano, J.S. Dolado, A. Ayuela, Aluminum incorporation to dreierketten silicate chains, J. Phys. Chem. B, 113 (9) (2009) 2832-2839.

[16] M.J. Abdolhosseini Qomi, F.J. Ulm, R.J.M. Pellenq, Evidence on the dual nature of aluminum in the calcium-silicate-hydrates based on atomistic simulations, J. Am. Ceram. Soc., 95 (3) (2012) 1128-1137.

[17] R.J. Myers, S.A. Bernal, R. San Nicolas, J.L. Provis, Generalized structural description of calcium-sodium aluminosilicate hydrate gels: the cross-linked substituted tobermorite model, Langmuir, 29 (2013) 5294-5306.

[18] S. Merlino, E. Bonaccorsi, T. Armbruster, The real structure of tobermorite 11Å: normal and anomalous forms, OD character and polytypic modifications, Eur. J. Mineral., 13 (3) (2001) 577-590.

[19] G.K. Sun, J.F. Young, R.J. Kirkpatrick, The role of Al in C-S-H: NMR, XRD, and compositional results for precipitated samples, Cem. Concr. Res., 36 (1) (2006) 18-29.

[20] X. Pardal, I. Pochard, A. Nonat, Experimental study of Si-Al substitution in calcium-silicate-hydrate (C-S-H) prepared under equilibrium conditions, Cem. Concr. Res., 39 (8) (2009) 637-643.

[21] E. L'Hôpital, B. Lothenbach, G. Le Saoût, D.A. Kulik, K. Scrivener, Incorporation of aluminium in calcium-silicate-hydrates, Cem. Concr. Res., submitted (2014).

[22] J.J. Chen, J.J. Thomas, H.F.W. Taylor, H.M. Jennings, Solubility and structure of calcium silicate hydrate, Cem. Concr. Res., 34 (9) (2004) 1499-1519.

[23] C.S. Walker, D. Savage, M. Tyrer, K.V. Ragnarsdottir, Non-ideal solid solution aqueous solution modeling of synthetic calcium silicate hydrate, Cem. Concr. Res., 37 (4) (2007) 502-511.

[24] B. Lothenbach, L. Pelletier-Chaignat, F. Winnefeld, Stability in the system CaO–Al_2O_3–H_2O, Cem. Concr. Res., 42 (12) (2012) 1621-1634.

[25] B.H. O'Connor, M.D. Raven, Application of the Rietveld refinement procedure in assaying powdered mixtures, Powder Diffr., 3 (1) (1988) 2-6.

[26] D.A. Kulik, T. Wagner, S.V. Dmytrieva, G. Kosakowski, F.F. Hingerl, K.V. Chudnenko, U. Berner, GEM-Selektor geochemical modeling package: revised algorithm and GEMS3K numerical kernel for coupled simulation codes, Comput. Geosci., 17 (1) (2013) 1-24.

[27] T. Wagner, D.A. Kulik, F.F. Hingerl, S.V. Dmytrieva, GEM-Selektor geochemical modeling package: TSolMod library and data interface for multicomponent phase models, Can. Mineral., 50 (5) (2012) 1173-1195.

[28] T. Thoenen, W. Hummel, U. Berner, The PSI/Nagra Chemical Thermodynamic Database 12/07: present status and future developments, Mineral. Mag., 77 (5) (2013) 2327.

[29] W. Hummel, U. Berner, E. Curti, F.J. Pearson, T. Thoenen, Nagra/PSI Chemical Thermodynamic Database 01/01, Universal Publishers, Parkland, 2002.

[30] D.A. Kulik, M. Kersten, Aqueous solubility diagrams for cementitious waste stabilization systems: II. End-member stoichiometries of ideal calcium silicate hydrate solid solutions, J. Am. Ceram. Soc., 84 (12) (2001) 3017-3026.

[31] B. Lothenbach, F. Winnefeld, Thermodynamic modelling of the hydration of Portland cement, Cem. Concr. Res., 36 (2) (2006) 209-226.

[32] G. Möschner, B. Lothenbach, J. Rose, A. Ulrich, R. Figi, R. Kretzschmar, Solubility of Fe–ettringite ($Ca_6[Fe(OH)_6]_2(SO_4)_3 \cdot 26H_2O$), Geochim. Cosmochim. Acta, 72 (1) (2008) 1-18.

[33] G. Möschner, B. Lothenbach, F. Winnefeld, A. Ulrich, R. Figi, R. Kretzschmar, Solid solution between Al-ettringite and Fe-ettringite ($Ca_6[Al_{1-x}Fe_x(OH)_6]_2(SO_4)_3 \cdot 26H_2O$), Cem. Concr. Res., 39 (6) (2009) 482-489.

[34] T. Schmidt, B. Lothenbach, M. Romer, K. Scrivener, D. Rentsch, R. Figi, A thermodynamic and experimental study of the conditions of thaumasite formation, Cem. Conc. Res., 38 (3) (2008) 337-349.

[35] D.A. Kulik, M. Kersten, Aqueous solubility diagrams for cementitious waste stabilization systems. 4. A carbonation model for Zn-doped calcium silicate hydrate by Gibbs energy minimization, Environ. Sci. Technol., 36 (13) (2002) 2926-2931.

[36] B.Z. Dilnesa, B. Lothenbach, G. Renaudin, A. Wichser, D. Kulik, Synthesis and characterization of hydrogarnet $Ca_3(Al_xFe_{1-x})_2(SiO_4)_y(OH)_{4(3-y)}$, Cem. Concr. Res., 59 (2014) 96-111.

[37] H.C. Helgeson, D.H. Kirkham, G.C. Flowers, Theoretical prediction of the thermodynamic behavior of aqueous electrolytes at high pressures and temperatures: IV. Calculation of activity coefficients, osmotic coefficients, and apparent molal and standard and relative partial molal properties to 600°C and 5 kb, Am. J. Sci., 281 (10) (1981) 1249-1516.

[38] S. Grangeon, F. Claret, Y. Linard, C. Chiaberge, X-ray diffraction: a powerful tool to probe and understand the structure of nanocrystalline calcium silicate hydrates, Acta Crystallogr. B, 69 (5) (2013) 465-473.

[39] A.C.A. Muller, K.L. Scrivener, A.M. Gajewicz, P.J. McDonald, Use of bench-top NMR to measure the density, composition and desorption isotherm of C–S–H in cement paste, Micropor. Mesopor. Mat., 178 (2013) 99-103.

[40] A. Gmira, R.J.M. Pellenq, I. Rannou, L. Duclaux, C. Clinard, T. Cacciaguerra, N. Lequeux, H. Van Damme, A structural study of dehydration/rehydration of tobermorite, a model cement compound, in: F. Rodriguez-Reinoso, B. McEnaney, J. Rouquerol, K. Unger (Eds.), Characterization of porous solids VI: proceedings of the

6th international symposium on the characterization of porous solids (COPS-VI), Elsevier, Alicante, 2002, pp. 601-608.

[41] H.J. Kuzel, Crystallographic data and thermal decomposition of synthetic gehlenite hydrate $2CaO.Al_2O_3.SiO_2.8H_2O$, Nueus. Jb. Miner. Monat., 148 (1976) 319-325.

[42] F.J. Trojer, The crystal structure of parawollastonite, Z. Kristallogr., 127 (1-6) (1968) 291-308.

[43] G.L. Kalousek, Application of differential thermal analysis in a study of the system lime-silica-water, in: Proceedings of the Third International Symposium on the Chemistry of Cement, Cement and Concrete Association, London, 1952.

[44] T. Mitsuda, H.F.W. Taylor, Normal and anomalous tobermorites, Mineral. Mag., 42 (322) (1978) 229-235.

[45] P.S. Roller, G. Ervin, The system calcium oxide-silica-water at 30°C. The association of silicate ion in dilute alkaline solution, J. Am. Chem. Soc., 62 (3) (1940) 461-471.

[46] H.F.W. Taylor, Hydrated calcium silicates. Part I. Compound formation at ordinary temperatures, J. Chem. Soc., (1950) 3682-3690.

[47] S.A. Greenberg, T.N. Chang, Investigation of the colloidal hydrated calcium silicates. II. Solubility relationships in the calcium oxide-silica-water system at 25°C, J. Phys. Chem., 69 (1) (1965) 182-188.

[48] K. Fujii, W. Kondo, Heterogeneous equilibrium of calcium silicate hydrate in water at 30°C, J. Chem. Soc., Dalton Trans., (2) (1981) 645-651.

[49] M. Grutzeck, A. Benesi, B. Fanning, Silicon-29 magic angle spinning nuclear magnetic resonance study of calcium silicate hydrates, J. Am. Ceram. Soc., 72 (4) (1989) 665-668.

[50] H.M. Jennings, Refinements to colloid model of C-S-H in cement: CM-II, Cem. Concr. Res., 38 (3) (2008) 275-289.

[51] A.C.A. Muller, K.L. Scrivener, A.M. Gajewicz, P.J. McDonald, Densification of C–S–H measured by ^{1}H NMR relaxometry, J. Phys. Chem. C, 117 (1) (2013) 403-412.

[52] J. Skibsted, M.D. Andersen, The effect of alkali ions on the incorporation of aluminum in the calcium silicate hydrate (C–S–H) phase resulting from Portland cement hydration studied by ^{29}Si MAS NMR, J. Am. Ceram. Soc., 96 (2013) 651-656.

[53] I.G. Richardson, A.R. Brough, R. Brydson, G.W. Groves, C.M. Dobson, Location of aluminum in substituted calcium silicate hydrate (C-S-H) gels as determined by ^{29}Si and ^{27}Al NMR and EELS, J. Am. Ceram. Soc., 76 (9) (1993) 2285-2288.

[54] T.T.H. Bach, C. Cau dit Coumes, I. Pochard, C. Mercier, B. Revel, A. Nonat, Influence of temperature on the hydration products of low pH cements, Cem. Concr. Res., 42 (6) (2012) 805-817.

[55] S. Masse, H. Zanni, J. Lecourtier, J.C. Roussel, A. Rivereau, ^{29}Si solid state NMR study of tricalcium silicate and cement hydration at high temperature, Cem. Concr. Res., 23 (5) (1993) 1169-1177.

[56] S. Kwan, J. LaRosa, M.W. Grutzeck, ^{29}Si and ^{27}Al MAS NMR study of strätlingite, J. Am. Ceram. Soc., 78 (7) (1995) 1921-1926.

[57] I.G. Richardson, G.W. Groves, The incorporation of minor and trace elements into calcium silicate hydrate (C-S-H) gel in hardened cement pastes, Cem. Concr. Res., 23 (1) (1993) 131-138.

[58] C.L. Dickson, D.R.M. Brew, F.P. Glasser, Solubilities of CaO-SiO_2-H_2O phases at 25°, 55° and 85°C, Adv. Cem. Res., 16 (2004) 35-43.

[59] E.L. Shock, D.C. Sassani, M. Willis, D.A. Sverjensky, Inorganic species in geologic fluids: correlations among standard molal thermodynamic properties of aqueous ions and hydroxide complexes, Geochim. Cosmochim. Acta, 61 (5) (1997) 907-950.

[60] D.A. Sverjensky, E.L. Shock, H.C. Helgeson, Prediction of the thermodynamic properties of aqueous metal complexes to 1000°C and 5 kb, Geochim. Cosmochim. Acta, 61 (7) (1997) 1359-1412.

[61] E.L. Shock, H.C. Helgeson, D.A. Sverjensky, Calculation of the thermodynamic and transport properties of aqueous species at high pressures and temperatures: standard partial molal properties of inorganic neutral species, Geochim. Cosmochim. Acta, 53 (9) (1989) 2157-2183.

[62] J.W. Johnson, E.H. Oelkers, H.C. Helgeson, SUPCRT92: A software package for calculating the standard molal thermodynamic properties of minerals, gases, aqueous species, and reactions from 1 to 5000 bar and 0 to 1000°C, Comput. Geosci., 18 (7) (1992) 899-947.

[63] H.C. Helgeson, J.M. Delany, H.W. Nesbitt, Summary and critique of the thermodynamic properties of rock-forming minerals, Am. J. Sci., 278-A (1978).

[64] R.A. Robie, B.S. Hemingway, Thermodynamic properties of minerals and related substances at 298.15 K and 1 bar (10^5 Pascals) pressure and at higher temperatures, United States Government Printing Office, Washington D.C., 1995.

Appendix A. Relevant thermodynamic data

Thermodynamic properties of the aqueous species and solid phases used in GEM-Selektor to calculate *SI** and $\log_{10}(K_{so})$ values are shown in Tables A1-A3.

Table A1. Standard partial molal thermodynamic properties of the aqueous species used in the thermodynamic modelling calculations. The reference state is unit activity in a hypothetical one molal solution referenced to infinite dilution.

Preprint version of accepted article. Please cite as:
*R.J. Myers, E. L'Hôpital, J.L. Provis, B. Lothenbach, "Effect of temperature and aluminium on calcium (alumino)silicate hydrate chemistry under equilibrium conditions", Cement and Concrete Research **2015**, 68:83-93.*
Official journal version is online at http://dx.doi.org/10.1016/j.cemconres.2014.10.015

Species	V° (cm^3/mol)	$\Delta_f H°$ (kJ/mol)	$\Delta_f G°$ (kJ/mol)	S° (J/mol.K)	Cp° (J/mol.K)	Reference
Al^{3+}	-45.2	-530.6	-483.7	-325.1	-128.7	[59]
AlO^+ (+ H_2O = $Al(OH)_2^+$)	0.3	-713.6	-660.4	-113.0	-125.1	[59]
AlO_2^- (+ $2H_2O$ = $Al(OH)_4^-$)	9.5	-925.6	-827.5	-30.2	-49.0	[59]
$AlOOH^o$ (+ $2H_2O$ = $Al(OH)_3^o$)	13.0	-947.1	-864.3	20.9	-209.2	[59]
$AlOH^{2+}$	-2.7	-767.3	-692.6	-184.9	56.0	[59]
$AlHSiO_3^{2+}$ (+ H_2O = $AlSiO(OH)_3^{2+}$)	0	-1634.3	-1540.5	-25.0	-215.9	[28, 29]
$AlSiO_5^{3-}$ (+ $2H_2O$ = $AlSiO_3(OH)_4^{3-}$)	0	-2014.2	-1769.0	-66.3	-292.2	[28, 29]
Ca^{2+}	-18.4	-543.1	-552.8	-56.5	-30.9	[59]
$CaOH^+$	5.8	-751.6	-717.0	28.0	6.0	[59]
$Ca(HSiO_3)^+$ (+ H_2O = $CaSiO(OH)_3^+$)	-6.7	-1686.5	-1574.2	-8.3	137.8	[60]
$CaSiO_3^o$ (+ H_2O = $CaSiO_2(OH)_2^o$)	15.7	-1668.1	-1517.6	-136.7	88.9	[9]
K^+	9.0	-252.1	-282.5	101.0	8.4	[59]
KOH^o	15.0	-474.1	-437.1	108.4	-85.0	[59]
Na^+	-1.2	-240.3	-261.9	58.4	38.1	[59]
$NaOH^o$	3.5	-470.1	-418.1	44.8	-13.4	[59]
$HSiO_3^-$ (+ H_2O = $SiO(OH)_3^-$)	4.5	-1144.7	-1014.6	20.9	-87.2	[60]
SiO_2^o	16.1	-887.9	-833.4	41.3	44.5	[30, 61]
$SiO_4O_{10}^{4-}$ (+ $2H_2O$ = $Si_4O_8(OH)_4^{4-}$)	0	-4082.7	-3600.8	-253.9	-1123.2	[28, 29]
SiO_3^{2-} (+ H_2O = $SiO_2(OH)_2^{2-}$)	34.1	-1098.7	-938.5	-80.2	119.8	[9]
OH^-	-4.7	-230.0	-157.3	-10.7	-136.3	[59]
H^+	0	0	0	0	0	[59]
H_2O^o	18.1	-285.9	-237.2	69.9	75.4	[62]
N_2^o	33.4	-10.4	18.2	95.8	234.2	[61]
O_2^o	30.5	-12.2	16.4	109.0	234.1	[61]

Preprint version of accepted article. Please cite as:
*R.J. Myers, E. L'Hôpital, J.L. Provis, B. Lothenbach, "Effect of temperature and aluminium on calcium (alumino)silicate hydrate chemistry under equilibrium conditions", Cement and Concrete Research **2015**, 68:83-93.*
Official journal version is online at http://dx.doi.org/10.1016/j.cemconres.2014.10.015

Table A2. Standard partial molar thermodynamic properties of the solid phases used in the thermodynamic modelling calculations. The reference state is 298.15 K and 1 bar.

Phase	V ° (cm^3/mol)	$\Delta_f H°$ (kJ/mol)	$\Delta_f G°$ (kJ/mol)	S° (J/mol.K)	Cp° (J/mol.K)	Reference
$Al(OH)_3$ (microcrystalline)	32.0	-1265.3	-1148.4	140.0	93.1	[24]
Gibbsite	32.0	-1288.7	-1151.0	70.1	93.1	[63]
Portlandite	33.1	-984.7	-897.0	83.4	87.5	[64]
SiO_2 (amorphous)	29.0	-903.3	-848.9	41.3	44.5	[11]
Katoite, C_3AH_6	149.7	-5537.3	-5008.2	421.7	445.6	[24]
Si-hydrogarnet, $C_3AS_{0.84}H_{4.32}$	142.5	-5847.5	-5365.2	375.2	412.6	[36]
Strätlingite, C_2ASH_8	216.1	-6360.0	-5705.1	546.2	602.7	[9]
C-S-H solid solution, the 'downscaled CSH3T' model						
TobH - $(CaO)_1(SiO_2)_{1.5}(H_2O)_{2.5}$	85.0	-2833.0	-2562.0	152.8	231.2	[11]
T5C - $(CaO)_{1.25}(SiO_2)_{1.25}(H_2O)_{2.5}$	79.3	-2782.0	-2519.0	159.9	234.1	[11]
T2C - $(CaO)_{1.5}(SiO_2)_1(H_2O)_{2.5}$	80.6	-2722.0	-2467.0	167.0	237.0	[11]

Table A3. Dissociation constant reactions for the solid phases used in the thermodynamic modelling calculations.

Phase	Reaction	$\log_{10}(K_{so})$	Reference
$Al(OH)_3$ (microcrystalline)	$Al(OH)_3 + OH^- \rightleftharpoons AlO_2^- + 2H_2O$	-0.67	[24]
Gibbsite	$Al(OH)_3 + OH^- \rightleftharpoons AlO_2^- + 2H_2O$	-1.12	[28, 29]
Portlandite	$Ca(OH)_2 \rightleftharpoons Ca^{2+} + 2OH^-$	-5.20	[28, 29]
SiO_2 (amorphous)	SiO_2 (am) $\rightleftharpoons SiO(OH)_3^- - OH^- - H_2O$	1.476	[31]
Katoite, C_3AH_6	$(CaO)_3(Al_2O_3)(H_2O)_6 \rightleftharpoons 3Ca^{2+} + 2AlO_2^- + 4H_2O + 4OH^-$	-20.50	[24]
Si-hydrogarnet, $C_3AS_{0.84}H_{4.32}$	$(CaO)_3(Al_2O_3)(SiO_2)_{0.84}(H_2O)_{4.32} \rightleftharpoons 3Ca^{2+} + 2AlO_2^- + 2.32H_2O + 3.16OH^- + 0.84HSiO_3^-$	-26.70	[36]
Strätlingite, C_2ASH_8	$(CaO)_2(Al_2O_3)(SiO_2)(H_2O)_8 \rightleftharpoons 2Ca^{2+} + 2AlO_2^- + HSiO_3^- + 7H_2O + OH^-$	-19.70	[9]
C-S-H, $(CaO)_{1.25}(SiO_2)_{1.25}(H_2O)_{2.5}$	$(CaO)_{1.25}(SiO_2)_{1.25}(H_2O)_{2.5} \rightleftharpoons 1.25SiO(OH)_3^- + 1.25Ca^{2+} + 1.25OH^-$	-11.625	[11]